From the observed conditions *hkl*, *h* + *k* = 2*n*, and *h0l*, *l* = 2*n*, the two possible space groups are *Cc* (No. 9) and *C*2/*c* (No. 15). Solution of the structure was accomplished by Patterson methods. Both the anion and the cation can be located on crystallographic 2-fold axes. Thus *C*2/*c* is the space group of choice.

An absorption correction was applied.[30] Four low-angle reflections appeared to be affected by extinction and were removed from the set of reflections used in refinement. The lattice molecule of chloroform was disordered and was given an occupancy of 0.5 on the basis of Fourier peak heights. It was refined with inter-chlorine and chlorine–carbon distance constraints by the method of additional observational equations.[4] Another site in the lattice is occupied by two partial molecules of dichloromethane that are rotated approximately 90° with respect to their chlorine–chlorine vectors. They were refined with fixed *U*'s of 0.08 Å² and variable occupancies that converged at 0.309 (9) and 0.195 (9), respectively. Hydrogen atoms were included in the structure factor calcualtion at idealized positions by using a model in which the hydrogen atoms ride on the bonded carbon and C–H is 0.96 Å. In the final cycles

of refinement all non-hydrogen atoms were assigned anisotropic thermal parameters except the carbon of chloroform and the chlorines of dichloromethane (the latter carbon atom was not located). In the final difference map the largest feature was 2.1 e Å⁻³ in height, in the vicinity of one of the chloroform molecules.

X-ray Structure Determination and Refinement for 3. Orange blocks of Ru(dpma)₂Cl₂ were obtained by diffusion of methanol into a dichloromethane solution of the complex. Data collection, treatment, and refinement followed the procedures outlined for **2**. A value of 0.81 e Å⁻³ was found for the largest feature in the final difference map. This was 0.69 Å away from C(19).

Supplementary Material Available: Listings of all bond lengths, bond angles, hydrogen atom positions, anisotropic thermal parameters, and data collection parameters (10 pages); listings of observed and calculated structure factors (58 pages). Ordering information is given on any current masthead page.

(30) XABS produces an absorption tensor from an expression relating F_o and F_c: Moezzi, B. Ph.D. Thesis, University of California, Davis, CA, 1988.

Kinetic and Thermodynamic Stabilities of the Geometric Isomers of (R₃P)₂Ru(CO)₂Cl₂ and (R₃P)₃Ru(CO)Cl₂ Complexes

Daniel W. Krassowski,[1a] John H. Nelson,*,[1a] Kay R. Brower,[1b] Dale Hauenstein,[1c] and Robert A. Jacobson[1c]

A series of ruthenium(II) complexes of the type RuCl₂(CO)₂P₂ (P = Bzl₃P, Ph₃P, Ph₂MeP, PhMe₂P, Me₃P) have been prepared and characterized by elemental analyses, physical properties, infrared spectroscopy, UV–visible spectroscopy, and ¹H, ¹³C{¹H} and ³¹P{¹H} NMR spectroscopy. The first-formed complex, with all ligand pairs trans (*ttt*), thermally isomerizes in solution to produce the isomer with all ligand pairs cis (*ccc*). This *ccc* isomer further isomerizes in solution to produce the thermodynamically preferred isomer with only the phosphine ligands trans (*cct*). The size and basicity of the phosphine affect the isomerization rate, which increases with an increase in size and a decrease in phosphine basicity and proceeds by initial dissociation of carbon monoxide. Activation parameters, Δ*S*° and Δ*V*°, are both positive for the *ttt*–*ccc* isomerization consistent with a dissociative process. Negative values of Δ*S*° for the *ccc* → *cct* isomerization suggest that an associative step may be important. *cis*- and *trans*-RuCl₂(CO)P₃ complexes with meridionally coordinated phosphines (P = Me₃P, PhMe₂P, Ph₂MeP) were also prepared and characterized by the same methods. The first-formed isomer with trans chlorides thermally isomerizes in solution to the thermodynamically stable isomer with cis chlorides. Positive values of both Δ*S*° and Δ*V*° are consistent with a dissociative process. Phosphine inhibition of this isomerization indicates initial phosphine dissociation. The crystal structures of *cis*(1)- and *trans*-RuCl₂(CO)(Ph₂MeP)₃ (**1** and **2**, respectively) have been determined by counter methods. Compound **1** crystallizes in space group *P*1̄ with *a* = 16.158 (4) Å, *b* = 18.361 (3) Å, *c* = 13.170 (4) Å, α = 93.36 (2)°, β = 108.03 (3)°, γ = 90.75 (2)°, and *Z* = 4. Compound **2** crystallizes in space group *P*2₁/*c* with *a* = 20.373 (9) Å, *b* = 9.831 (5) Å, *c* = 20.689 (7) Å, β = 117.43 (3)°, and *Z* = 4. Both structures were refined by least-squares methods with *R* = 0.093 for **1** and *R* = 0.069 for **2** for 4614 and 2974 unique reflections with *I*/σ(*I*) ≥ 3.0 for **1** and **2**, respectively. The bond distance of the phosphine trans to carbon monoxide in the trans isomer (*d*(RuP) = 2.490 (4) Å) is longer than the other two Ru–P distances (2.403 (4) Å). The ³¹P{¹H} NMR data also suggest that this phosphine is relatively weakly bound and so this phosphine likely dissociates as the first step in the geometric isomerization.

Introduction

Following the simultaneous discovery by Wilkinson[2] and Coffey[3] in 1965 of the catalytic homogeneous hydrogenation of terminal alkenes by RhCl(Ph₃P)₃ under mild conditions, the catalytic reduction of unsaturated organic substrates by transition-metal phosphine complexes has been extensively studied and recently reviewed.[4,5] It is now widely accepted that in order for a metal complex to act as a homogeneous catalyst, there must be a vacant coordination site available on the metal for binding the substrate. For this reason coordinatively unsaturated complexes are especially

effective catalysts. Both RhCl(Ph₃P)₃[6] and RuCl₂(Ph₃P)₃,[7–9] which are among the most active homogeneous hydrogenation catalysts known,[5] are 16-electron species and further dissociate at least one phosphine ligand in solution.

On the other hand, coordinatively saturated complexes must first dissociate a ligand in order to gain entry into a catalytic cycle. As a consequence, catalytic activity may be related to the ease of ligand dissociation. We report here that complexes of the type *trans*-RuCl₂(CO)P₃ (P = tertiary phosphine) dissociate a phosphine ligand in the course of their geometric isomerization to the thermodynamically preferred cis isomers. Similarly, complexes of the type *ttt*-RuCl₂(CO)₂P₂ have been found to thermally isomerize but by CO dissociation.[10–13] We anticipated that there

(1) (a) University of Nevada. (b) New Mexico Institute of Mining and Technology. (c) Iowa State University.
(2) Young, J. F.; Osborn, J. A.; Jardine, F. H.; Wilkinson, G. *Chem. Commun.* **1965**, 131.
(3) Coffey, R. S. Br. Patent No. 1 121 642, Feb 18, 1965.
(4) James, B. R. *Homogeneous Hydrogenation*; Wiley: New York, 1973.
(5) Pignolet, L. H. *Homogeneous Catalysis with Metal Phosphine Complexes*; Plenum: New York, 1983.

(6) Halpern, J.; Wong, C. S. *J. Chem. Soc., Chem. Commun.* **1973**, 629.
(7) James, B. R.; Markham, L. O. *Inorg. Chem.* **1974**, *13*, 97.
(8) Halmann, P. S.; McGarvey, B. R.; Wilkinson, G. *J. Chem. Soc. A* **1968**, 3143.
(9) Stephenson, T. A.; Wilkinson, G. *J. Inorg. Nucl. Chem.* **1966**, *28*, 945.

might be a relationship between the catalytic activity of these species and the rates and mechanisms of their geometric isomerization. Thus, we have investigated in detail the kinetics of these geometric isomerizations.

Experimental Section

(A) Reagents and Physical Measurements. All chemicals were reagent grade and were used as received or synthesized as described below. The phosphines were purchased from Strem Chemicals, Inc. (*Caution*: Me$_3$P is flammable in air and must be handled under nitrogen.) The other phosphines are mildly air-sensitive and can usually be exposed briefly to the atmosphere without significant oxidation. Chloroform, chlorobenzene, and *sym*-tetrachloroethane were purified by standard procedures[14] and distilled just prior to use for kinetic studies. Melting points were determined on a Mel-Temp apparatus and are uncorrected. Infrared spectra were obtained on a Perkin-Elmer 599 spectrometer, as Nujol mulls between CsBr windows, as chloroform or tetrachloroethane solutions in 0.1-mm sealed NaCl cells, or as CsI pellets. The ^{1}H, ^{31}P{^{1}H}, and ^{13}C{^{1}H} NMR spectra were recorded at 99.54, 40.26, and 25.00 MHz, respectively, on a JEOL-FX-100 spectrometer in the FT mode. Proton and carbon chemical shifts are relative to that of internal Me$_4$Si, while the phosphorus chemical shifts are relative to that of external 85% H$_3$PO$_4$, with a positive value being downfield of the respective reference. Visible spectra were obtained by using a Cary 14 spectrophotometer on chlorobenzene solutions of the complexes contained in a 5.0-cm quartz cell.

(B) Synthesis. *ttt*-RuCl$_2$(CO)$_2$P$_2$ (P = Ph$_2$MeP, PhMe$_2$P, Bzl$_3$P). The preparation of *ttt*-RuCl$_2$(CO)$_2$(Ph$_2$MeP)$_2$ is described in detail. The other two all-trans complexes were prepared similarly. Carbon monoxide was bubbled for 5 h through a refluxing solution of RuCl$_3$·3H$_2$O (2.43 g, 9.30 mmol) in 50 mL of absolute ethanol. The resulting deep red solution was cooled to 0 °C and stirred magnetically while a solution containing 3.83 g (19.1 mmol) of Ph$_2$MeP in 30 mL of freshly distilled chloroform was added dropwise. With carbon monoxide still passing through the red solution (green for the preparations of the PhMe$_2$P and Bzl$_3$P complexes), stirring was continued until the solution turned yellow and a precipitate formed (about 15 min). The precipitate was isolated by filtration, washed with absolute ethanol and anhydrous diethyl ether, and vacuum-dried overnight.

ttt-RuCl$_2$(CO)$_2$(Me$_3$P)$_2$. Carbon monoxide was bubbled through a refluxing solution of 2.65 g (10.1 mmol) of RuCl$_3$·3H$_2$O in 100 mL of 2-methoxyethanol for 24 h to produce a bright yellow solution. A modified Dean–Stark trap was then used to remove 70 mL of the solvent, and the remaining light orange solution was cooled in a dry-ice/acetone bath. To this solution was added a solution containing 2.1 mL (1.6 g, 21 mmol) of Me$_3$P in 5 mL of 2-methoxyethanol by syringe. The resulting darker orange solution was allowed to warm to room temperature, and 25 mL of solvent was removed at 3.5 Torr (40 °C). After addition of 1 mL of absolute ethanol and 50 mL of anhydrous diethyl ether a yellow precipitate formed. This was separated by filtration, washed with anhydrous diethyl ether, and vacuum-dried overnight. A second crop of this complex was isolated from the filtrate following the addition of a small amount of water and overnight cooling in a refrigerator. The two crops were combined and recrystallized from dichloromethane/methanol.

ccc-RuCl$_2$(CO)$_2$(Ph$_2$MeP)$_2$. A suspension of 0.283 g of [RuCl$_2$-(CO)(Ph$_2$MeP)$_2$]$_2$ (vide infra) in 30 mL of freshly distilled chloroform was placed in a thick-walled 90-mL Fischer–Porter pressure vessel. The vessel was sealed, and carbon monoxide was bubbled through the suspension for 4 min. The system was then pressurized to 40 psi with carbon monoxide, and the solution was stirred magnetically at room temperature for 20 h. The clear, colorless solution thus obtained was filtered, and the chloroform was removed under vacuum at 20 °C. The resulting colorless oil was dissolved in anhydrous diethyl ether and taken to dryness at 20 °C under reduced pressure to give the product.

ccc-RuCl$_2$(CO)$_2$(PhMe$_2$P)$_2$. Carbon monoxide was bubbled for 1 h through a suspension of 0.159 g of [RuCl$_2$(CO)(PhMe$_2$P)$_2$]$_2$ (vide infra) in 200 mL of acetone and 10 mL of chloroform. The solvent was then

removed from the clear colorless solution under reduced pressure at 20 °C to give the product.

cct-RuCl$_2$(CO)$_2$(Ph$_2$MeP)$_2$ and [RuCl$_2$(CO)(Ph$_2$MeP)$_2$]$_2$. A saturated solution containing 4.76 g of *ttt*-RuCl$_2$(CO)$_2$(Ph$_2$MeP)$_2$ in 20 mL of chloroform was refluxed for 27 h. The yellow [RuCl$_2$(CO)(Ph$_2$MeP)$_2$]$_2$ (2.16 g, mp 275–277 °C) that precipitated was isolated by filtration and washed with anhydrous diethyl ether. Absolute ethanol (20 mL) was added to the original orange filtrate, and this solution was left standing at room temperature overnight. The white needles that formed were isolated by filtration and recrystallized from chloroform/ethanol.

cct-RuCl$_2$(CO)$_2$(Bzl$_3$P)$_2$. A solution containing 0.712 g of *ttt*-RuCl$_2$(CO)$_2$(Bzl$_3$P)$_2$ in 4 mL of chloroform was refluxed for 2 h. The solution was cooled to room temperature, and 10 mL of absolute ethanol was added to cause precipitation of fine white needles from the yellow solution. The chloroform was removed under reduced pressure, and the crystals were isolated by filtration. The product was recrystallized from chloroform/ethanol.

cct-RuCl$_2$(CO)$_2$(PhMe$_2$P)$_2$. Carbon monoxide was bubbled through a refluxing solution containing 1.16 g (4.44 mmol) of RuCl$_3$·3H$_2$O in 25 mL of 2-methoxyethanol for 5 h to produce a bright yellow solution. To this solution was added a solution containing 1.25 g (9.10 mmol) of PhMe$_2$P in 25 mL of 2-methoxyethanol, and refluxing was continued for an additional 21 h. The solution was then taken to dryness under vacuum to give a yellow oil. The oil was triturated with absolute ethanol to produce an off-white powder, which was separated by filtration, washed with ethanol, and vacuum-dried overnight.

cct-RuCl$_2$(CO)$_2$(Me$_3$P)$_2$. Carbon monoxide was bubbled through a refluxing solution containing 3.07 g (11.7 mmol) of RuCl$_3$·3H$_2$O in 150 mL of 2-methoxyethanol for 14 h to produce a bright yellow solution. This solution was cooled to 0 °C, and a solution containing 2.60 mL (1.94 g, 25.5 mmol) of Me$_3$P in 5 mL of 2-methoxyethanol was added dropwise with stirring. No color change was apparent during the addition of the phosphine-containing solution. Carbon monoxide was bubbled through this solution for 16 h, and all but 5 mL of the solvent was then removed under vacuum (3 Torr) at 40 °C. The resulting solution was left standing at room temperature overnight. The off-white crystals that formed were isolated by filtration, washed with anhydrous diethyl ether, and vacuum-dried overnight.

ccc-RuCl$_2$(CO)$_2$(Ph$_3$P)$_2$. Carbon monoxide was bubbled through a refluxing solution containing 2.61 g (10.0 mmol) of RuCl$_3$·3H$_2$O in 50 mL of 2-methoxyethanol for 4 h to produce a bright yellow solution. After addition of 5.24 g (20.0 mmol) of Ph$_3$P and removal of 25 mL of solvent with the aid of a Dean–Stark trap, the solution was cooled to room temperature. The precipitate that formed was isolated by filtration, washed with ethanol, and vacuum-dried overnight.

[RuCl$_2$(CO)(Bzl$_3$P)$_2$]$_2$. A saturated solution containing 0.712 g of *ttt*-RuCl$_2$(CO)$_2$(Bzl$_3$P)$_2$ in 4 mL of chloroform was refluxed for 2 h. This solution was cooled to room temperature, 20 mL of absolute ethanol was added, and the white crystals of *cct*-RuCl$_2$(CO)$_2$(Bzl$_3$P)$_2$ that precipitated were isolated by filtration. The yellow filtrate was then taken to dryness under vacuum. The crude yellow product thus obtained was recrystallized by dissolving it in 3 drops of chloroform and adding anhydrous diethyl ether (10 mL). Slow evaporation of this solution at ambient temperature gave the dimer as a yellow powder: yield 0.023 g (3%); mp 95–115 °C.

[RuCl$_2$(CO)(PhMe$_2$P)$_2$]$_2$. Carbon monoxide was bubbled through a refluxing solution of 1.51 g (5.78 mmol) of RuCl$_3$·3H$_2$O in 125 mL of 2-methoxyethanol for 5 h to produce a clear yellow solution. To this solution was added a solution containing 1.66 g (12.0 mmol) of PhMe$_2$P in 20 mL of 2-methoxyethanol, and the resulting solution was refluxed overnight. After 70 mL of solvent was removed with a modified Dean–Stark trap, the yellow solution was cooled to room temperature, filtered, and allowed to slowly evaporate at ambient temperature for 6 weeks. The remainder of the solvent was then removed under reduced pressure to give a yellow solid, which was washed with anhydrous diethyl ether and air-dried: yield 1.20 g (40%); mp 248–251 °C.

trans-RuCl$_2$(CO)(PhMe$_2$P)$_3$. This complex was prepared by the method of Jenkins et al.:[15] mp 163–165 °C (lit.[15] mp 164–165 °C).

cis-RuCl$_2$(CO)(PhMe$_2$P)$_3$. A solution containing 1.50 g of *trans*-RuCl$_2$(CO)(PhMe$_2$P)$_3$ in 25 mL of 2-methoxyethanol was refluxed for 3 h. The resulting yellow solution was reduced to 5 mL under vacuum to give a white precipitate. This was isolated by filtration and washed with anhydrous diethyl ether: yield 1.07 g (71%); mp 177–180 °C (lit.[15] 179–181 °C).

trans-RuCl$_2$(CO)(Ph$_2$MeP)$_3$. Carbon monoxide was bubbled through a refluxing solution of 1.30 g (4.9 mmol) of RuCl$_3$·3H$_2$O in 25 mL of absolute ethanol for 7 h. The resulting clear red solution was cooled to

(10) Wilkes, L. M.; Nelson, J. H.; Mitchener, J. P.; Babich, M. W.; Riley, W. C.; Helland, B. J.; Jacobson, R. A.; Cheng, M. Y.; Seff, K.; McCusker, L. B. *Inorg. Chem.* **1982**, *21*, 1376.

(11) Barnard, C. F. J.; Daniels, J. A.; Jeffrey, J.; Mawby, R. J. *J. Chem. Soc., Dalton Trans.* **1976**, 953.

(12) Gill, D. F.; Mann, B. E.; Shaw, B. S. *J. Chem. Soc., Dalton Trans.* **1973**, 311.

(13) Wilkes, L. M.; Nelson, J. H.; McCusker, L. B.; Seff, K.; Mathey, F. *Inorg. Chem.* **1983**, *22*, 2476.

(14) Riddick, J. A.; Bunger, W. B.; Sakano, T. K. *Organic Solvents, Physical Properties and Methods of Purification*, 4th ed.; Wiley-Interscience: New York, 1986.

(15) Jenkins, J. M.; Lupin, M. S.; Shaw, B. L. *J. Chem. Soc.* **1966**, 1787.

Table I. Physical Properties and Infrared Data for $RuCl_2(CO)_2(phosphine)_2$ Complexes

complex	geometry	color	ν_{CO},[a] cm^{-1}	ν_{RuCl},[b] cm^{-1}	% yield	mp, °C
$RuCl_2(CO)_2(Bzl_3P)_2$	*ttt*	yellow	2007	326	73	*d*
	ccc	NI[e]	2078, 2003			
	cct	white	2052, 1994	300, 276	84	227–229
$RuCl_2(CO)_2(Ph_3P)_2$	*cct*	white	2059, 1999	300, 270	96	309–312
$RuCl_2(CO)_2(Ph_2MeP)_2$	*ttt*	yellow	2011	332	63	152–157
	ccc	pale yellow	2087, 2000	305, 280	48	90
	cct	white	2056, 1996	309, 284	5	228–230
$RuCl_2(CO)_2(PhMe_2P)_2$	*ttt*	yellow	2008	326	53	139–142
	ccc	pale yellow	2081, 1998	299, 277	82	*d*
	cct	off-white	2053, 1995	306, 284	80	134–135
$RuCl_2(CO)_2(Me_3P)_2$	*ttt*	yellow	2006	341	23	*d*
	ccc	NI	2084, 1984[c]			
	cct	pale yellow	2050, 1986	315, 290	14	198–202

[a] As CHCl₃ solutions. [b] As CsI pellets. [c] Estimated; low-energy band obscured by *cct* isomer. [d] Isomerizes in the solid state at about 160 °C. [e] NI = not isolated.

0 °C, and 3.19 g (16.0 mmol) of Ph₂MeP was added by syringe to cause immediate precipitation of an orange solid. Chloroform (150 mL) was added to dissolve this precipitate, and the red solution was placed in a refrigerator. After 5 days the color of the solution had changed to orange. The solvent was removed under reduced pressure at ambient temperature until a precipitate just began to form. Further slow evaporation of the solvent in a refrigerator gave the product as orange crystals. These were isolated by filtration, washed with anhydrous diethyl ether, and air-dried: yield 1.44 g (36%); isomerizes to cis at ~165 °C.

***cis*-RuCl₂(CO)(Ph₂MeP)₃.** Carbon monoxide was bubbled through a refluxing solution of 1.52 g (5.81 mmol) of RuCl₃·3H₂O in 25 mL of absolute ethanol for 6 h. To the resulting clear red solution was added a solution containing 6.4 g (31.9 mmol) of Ph₂MeP in 50 mL of chloroform. The refluxing solution quickly turned orange and then yellow, and reflux was continued overnight. The solvent was then removed under reduced pressure to give a viscous yellow oil. Trituration of this oil with anhydrous diethyl ether gave a yellow powder. The crude complex was recrystallized from chloroform/ethanol to give the cis complex as small, bright yellow crystals: yield 2.33 g (48%); mp 238–244 °C.

***trans*-RuCl₂(CO)(Me₃P)₃.** Carbon monoxide was bubbled through a refluxing solution of 3.07 g (11.7 mmol) of RuCl₃·3H₂O in 150 mL of 2-methoxyethanol for 14 h. The resulting clear yellow solution was cooled to 0 °C, and 3.6 mL (2.7 g, 35.5 mmol) of Me₃P was added with a syringe. A gas was evolved, and the solution turned orange. This solution was stirred magnetically under nitrogen at ambient temperature for 16 h, and then the solution volume was decreased to 5 mL under vacuum at ambient temperature. The solution was then left standing at ambient temperature overnight, and large orange crystals formed. These were isolated by filtration, washed with anhydrous diethyl ether, and air-dried. This product (0.86 g) was identified by ³¹P NMR to be *ttt*-RuCl₂(CO)₂(Me₃P)₂. Addition of distilled water to the filtrate resulted in the precipitation of a fine yellow powder. This product was isolated by filtration, washed with anhydrous diethyl ether, and air-dried. A ³¹P NMR spectrum showed it to be pure *trans*-RuCl₂(CO)(Me₃P)₃: yield 2.10 g (42%); the complex did not melt but isomerized to the cis isomer in the solid state upon heating to ~160 °C.

***cis*-RuCl₂(CO)(Me₃P)₃.** The above trans isomer (0.4 g) was heated in an oven at 170 °C, turning from orange to light brown after 10 min. A ³¹P{¹H} NMR spectrum (CDCl₃) showed that the product was greater than 98% *cis*-RuCl₂(CO)(Me₃P)₃. This was washed with a small amount of anhydrous diethyl ether and air-dried: yield 0.38 g (95%); mp 230–233 °C.

Satisfactory carbon and hydrogen analyses were obtained for all compounds (Galbraith Laboratories, Knoxville, TN 37921). The percent yields and physical properties of the complexes are given in Table I.

(C) Kinetic Studies. Both visible and infrared spectroscopy were used to monitor the geometric isomerization of the *trans*-RuCl₂(CO)P₃ and *ttt*-RuCl₂(CO)₂P₂ complexes. The isomerizations of the near-colorless *ccc*-RuCl₂(CO)₂P₂ complexes were followed only by infrared spectroscopy. The methods used for monitoring the isomerizations of the specific complexes are given in Table II (supplementary material).

For the reactions followed by infrared spectroscopy, enough starting material to give a solution ca. 5.5 mM in complex was added to 25 mL of distilled chloroform or 1,1,2,2-tetrachloroethane that had been brought to the appropriate temperature in a Brinkman-Lauda K-2/R circulating temperature controller. The solution was contained in a 50-mL two-neck round-bottom flask with one neck sealed with a rubber septum and the other neck surmounted by a water-cooled condenser. The temperature variation of the bath was no greater than ±0.2 °C. The geometric

isomerization of the complexes was monitored by observing the decrease in the intensity of the following carbonyl absorptions: *ttt* complexes, ca. 2020 cm⁻¹; *ccc* complexes, ca. 2080 cm⁻¹; *trans*-RuCl₂(CO)P₃ complexes, ca. 1990 cm⁻¹. Aliquots of the reaction mixture were withdrawn at measured time intervals with a syringe and injected into NaCl solution cells (0.1 mm path length). The infrared spectra were recorded from 2140 to 1940 cm⁻¹ for the isomerizations of the *ttt* and *ccc* complexes and from 2050 to 1900 cm⁻¹ for the *trans*-RuCl₂(CO)P₃ complexes on a Perkin-Elmer Model 599 infrared spectrometer. All the complexes were found to obey the Beer–Lambert law in the concentration ranges of the isomerizations (0–6 mM).

The rate constants (k) for the isomerizations were usually obtained from the slope of a plot of ln (absorbance) vs time for more than 2 half-lives. In cases where there was some curvature to this plot, k was estimated from the slope of the tangent to the curve at 1 half-life. All kinetic data are the average of at least three such experiments. The isomerization of *ccc*-RuCl₂(CO)₂(PhMe₂P)₂ was only followed to 1 half-life due to its slow isomerization (even at 119 °C).

Chlorobenzene solutions no more than 4 M in the complex were required in order to monitor the isomerizations of the trans and *ttt* complexes by visible spectroscopy. The quartz solution cell used for these studies had a path length of 5 cm and could hold about 7 mL. The sample cell was surrounded by a hollow Pyrex jacket equipped with an inlet and an outlet to allow for passage of the heat-transfer fluid from a Brinkman-Lauda K-2/R circulating temperature controller. It was found that the sample solution required about 5 min to reach thermal equilibrium once the flow was begun around the cell. The temperature of the solution inside the cell was measured with an Omega 450 AET chromel/constantan (type E) thermocouple. Temperature variation in the cell was ±0.8 °C.

The maximum absorption for the trans and *ttt* complexes in the visible spectrum was found by scanning from 6500 to 3500 Å at a rate of 100 Å/5 s with a Cary-14 spectrophotometer. The spectrophotometer was then set to this maximum wavelength during the isomerization. Once heating of the cell had begun, no measurements were recorded until the cell had reached thermal equilibrium. After that time measurements were taken at timed intervals merely by turning on the master switch of the spectrophotometer. Reactions with excess phosphine were conducted under a prepurified N₂ atmosphere with freshly distilled phosphine, the purity of which was checked by ¹H and ³¹P NMR spectroscopy.

The rate constants for the isomerizations were found from plots of ln (absorbance) vs time to more than 2 half-lives. All kinetic data are the average of at least three such experiments.

(D) Activation Volume Measurements. Activation volumes were obtained by studying the effects of pressure (1–1360 bar) on the rates of geometric isomerization under the following conditions: *ttt*-RuCl₂(CO)₂(Ph₂MeP)₂ at 63.2 °C in *sym*-tetrachloroethane; *ttt*-RuCl₂(CO)₂(PhMe₂P)₂ at 70.4 °C in *sym*-tetrachloroethane; *trans*-RuCl₂(CO)(Ph₂MeP)₃ at 34.0 °C in chloroform; *trans*-RuCl₂(CO)(PhMe₂P)₃ at 64.3 °C in *sym*-tetrachloroethane. The high-pressure pump, gauge, valves, tubing, fittings, and micro series reactor were obtained from the American Instrument Co., Silver Springs, MD. The temperature of the reactor was controlled by a 100-kg aluminum ingot that was bored to fit the reactor body snugly. A thin oil film was used to improve thermal contact. The temperature of the ingot was controlled within 0.1 °C. Samples were contained in an inverted miniature glass bell that was sealed with mercury in contact with the pressure-transmitting fluid (glycol). After reaction for a measured period of time, usually several minutes, a portion of the sample was removed and placed directly in the

Table III. Crystal and Refinement Data for **1** and **2**[a]

	trans- $RuC_{40}H_{39}Cl_2OP_3$ (**1**)	*cis-* $RuC_{40}H_{39}Cl_2OP_3$ (**2**)
fw	800.64	800.64
a, Å	20.272 (9)	16.158 (4)
b, Å	9.831 (5)	18.361 (3)
c, Å	20.689 (7)	13.170 (4)
α, deg		93.36 (2)
β, deg	117.43 (3)	108.03 (3)
γ, deg		90.75 (2)
space group	$P2_1/c$	$P\bar{1}$
Z	4	4
d(calc), g/cm³	1.45	1.44
linear abs coeff, cm⁻¹	7.26	7.26
abs factor range	0.80–0.89	0.80–0.88
temp, K	298	298
final R_F	0.069	0.093
final R_{wF} ($w = 1/\sigma^2 F$)	0.68	0.122

[a] Stationary background counts were taken before and after the scan for 0.25 of the scan time; Mo Kα radiation; graphite monochromator; $\lambda = 0.710\,34$ Å (**1**) and $\lambda = 0.709\,79$ Å (**2**).

Table IV. Final Positional Parameters for the "Core" Atoms of cis-$(Ph_2MeP)_3Ru(CO)Cl_2$

atom	x	y	z
Ru1	0.7188 (2)[b]	0.7189 (1)	0.0130 (2)
Ru2	0.7828 (2)	0.2281 (1)	0.4623 (2)
Cl1	0.6490 (6)	0.8379 (4)	−0.0072 (6)
Cl2	0.5804 (5)	0.6565 (4)	−0.0820 (6)
Cl3	0.9274 (5)	0.1968 (4)	0.5780 (6)
Cl4	0.8332 (5)	0.3528 (4)	0.4418 (6)
P1	0.7929 (5)	0.6101 (4)	0.0375 (6)
P2	0.7233 (5)	0.7389 (4)	−0.1637 (6)
P3	0.6711 (5)	0.7083 (4)	0.1702 (6)
P4	0.7675 (5)	0.2791 (4)	0.6295 (6)
P5	0.7202 (5)	0.1147 (4)	0.4701 (6)
P6	0.8403 (5)	0.1972 (4)	0.3172 (6)
O1	0.8800 (13)	0.8075 (9)	0.1029 (15)
O2	0.6192 (12)	0.2731 (10)	0.3078 (15)
C79	0.8151 (20)	0.7719 (13)	0.0773 (24)

[a] The positional parameters are in fractional unit cell coordinates. [b] In this and succeeding tables, numbers in parentheses indicate standard deviations in the least significant figures.

IR liquid cell for analysis within 2 min. Duplicate experiments were performed at each pressure. Activation volumes were calculated from the slope of a plot of ln k vs P according to the equation $(\partial \ln k / \partial P)_T = -\Delta V^\ddagger / RT$ and have uncertainties of about ±1 mL.

(E) **Crystal Structure Analyses.** Crystals of *cis-* and *trans-*$RuCl_2$-$(CO)(Ph_2MeP)_3$ (**1** and **2**, respectively) were grown from nearly saturated solutions of the complexes in ethanol/chloroform. The solutions were sealed in 50-mL round-bottom flasks with rubber septa, and crystallization was induced by slow addition of anhydrous diethyl ether with a syringe. Crystal data and additional details of data collection and refinement are given in Table III. Intensity data were taken with a fully automated Datex four-circle X-ray diffractometer interfaced to an LSI 77/PDP-15 computer and operated in a real-time mode. Data were corrected for Lorentz[16] and polarization but, because of the small linear absorption coefficients, not for absorption. Systematic absences ($h0l$, $l \neq 2n$; $0k0$, $k \neq 2n$) indicated space group $P2_1/c$ for **1**, and no systematic absences were found for **2**. The heavy atoms were located by Patterson

(16) Structure factor calculations and least-squares refinements were done by using the block-matrix/full-matrix program ALLS (Lapp, R. L.; Jacobson, R. A. U.S. Department of Energy Report IS-4708; Iowa State University: Ames, IA, 1979), Fourier series calculations were done by using the program FOUR (Powell, D. R.; Jacobson, R. A. U.S. Department of Energy Report IS-4737; Iowa State University: Ames, IA, 1980), and for molecular drawings the program ORTEP (Johnson, C. K. U.S. Atomic Energy Commission Report ORNL-3794; Oak Ridge National Laboratory: Oak Ridge, TN, 1970) was used. Automatic indexing and crystal system determination were done by using ALICE (Jacobson, R. A. *J. Appl. Crystallogr.* **1976**, *9*, 115). Atomic scattering factors were those from: *International Tables for X-ray Crystallography*; Kynoch: Birmingham, England, 1974; Vol. IV, pp 71–99, 215–216. The ruthenium scattering factors were modified for the real and imaginary parts of anomalous dispersion.

Table V. Final Positional Parameters[a] for the "Core" Atoms of $trans$-$(Ph_2MeP)_3Ru(CO)Cl_2$

atom	x	y	z
Ru	0.2209 (1)	0.4985 (1)	0.4378 (1)
Cl1	0.2213 (2)	0.3843 (4)	0.3343 (2)
Cl2	0.2229 (2)	0.6033 (4)	0.5447 (2)
P1	0.3037 (2)	0.3289 (4)	0.5174 (2)
P2	0.3241 (2)	0.6318 (4)	0.4364 (2)
P3	0.1273 (2)	0.6579 (4)	0.3628 (2)
C40	0.1426 (7)	0.3862 (15)	0.4263 (7)
O1	0.0982 (6)	0.3195 (12)	0.4168 (6)

[a] The positional parameters are in fractional unit cell coordinates.
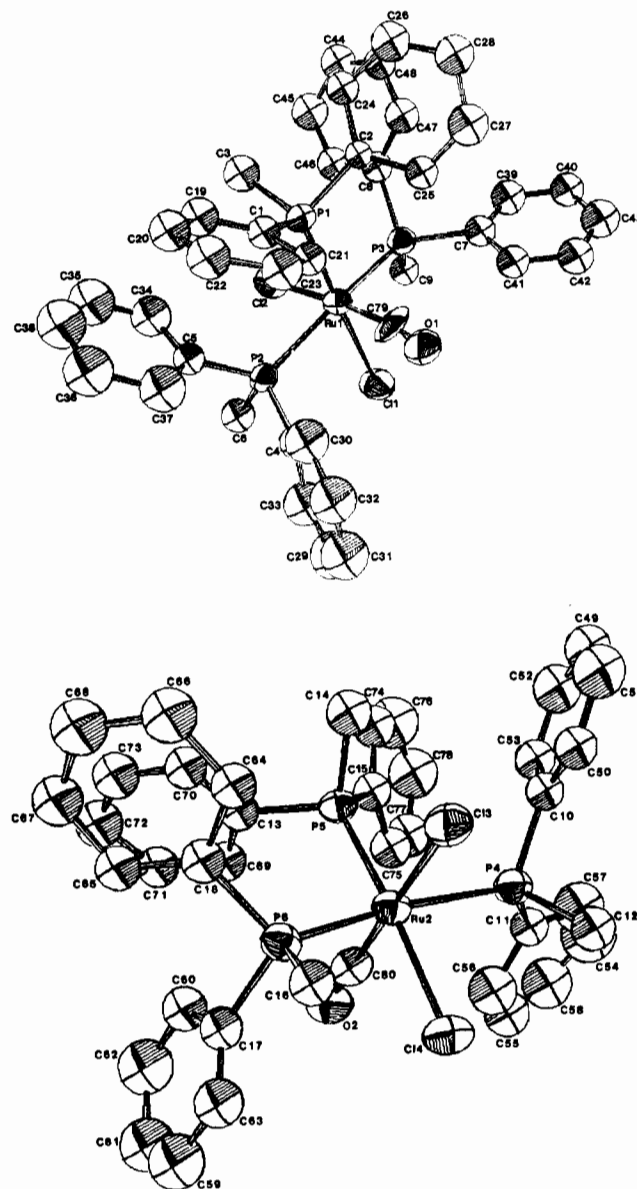
Figure 1. OREP diagram of cis-$(Ph_2MeP)_3Ru(CO)Cl_2$ with 50% probability ellipsoids showing the atom-numbering scheme. Selected bond distances (in Å) as average values for the two independent molecules are as follows: RuCl1, 2.461 (8); RuCl2, 2.454 (8); RuP1, 2.327 (7); RuP2, 2.407 (8); RuP3, 2.433 (8); RuC, 1.783 (29); CO, 1.167 (34). Average selected bond angles (in degrees) are as follows: Cl1RuCl2, 91.8 (3); Cl1RuP1, 86.2 (3); Cl1RuP2, 82.3 (3); Cl1RuP3, 175.1 (3); Cl1RuC, 84.0 (9); Cl2RuP1, 83.6 (9); Cl2RuP2, 84.3 (3); Cl2RuP3, 93.2 (3); Cl2RuC, 174.5 (9); P1RuP2, 163.1 (3); P1RuP3, 94.3 (3); P1RuC, 99.1 (9); P2RuP3, 98.3 (3); P2RuC, 92.1 (10); P3RuC, 91.1 (8).

techniques, and the light atoms were then found on successive Fourier syntheses. Hydrogen atoms were inserted at calculated positions (d(CH) = 1.05 Å) with fixed isotropic temperature factors (4.0 Å²)[16] and were not refined. Final refinement was by least-squares methods (minimizing $\sum w(|F_o| - |F_c|)^2$) in cascaded large blocks.[16] For **2** all non-hydrogen

Table VI. ^{1}H and ^{31}P{^{1}H} Nuclear Magnetic Resonance Data for RuCl$_2$(CO)$_2$(phosphine)$_2$ Complexes

		δ (mult^c) [J, Hz]	
phosphine	geometry	^{1}H, Me region^a	^{31}P{^{1}H}^{b}
Bzl$_3$P	ttt	3.53 (T) [6.4]^d	18.10 (s)
	ccc	NO	35.24 (d), 4.84 (d) [24.4]
	cct	3.57 (T) [7.1]^d	16.77 (s)
Ph$_3$P	ccc	NA	45.89 (d), 26.78 (d) [24.4]
	cct	NA	16.32 (s)
Ph$_2$MeP	ttt	2.21 (T) [7.6]	7.93 (s)
	ccc	2.25 (d) [10.5]; 1.54 (d) [10.7]	22.22 (d), 4.96 (d) [29.1]
	cct	2.31 (T) [8.9]	11.81 (s)
PhPMe$_2$	ttt	1.96 (T) [7.8]	−2.85 (s)
	ccc	1.94 (d) [10.5] (6 H); 1.60 (d) [10.5] (3 H); 1.43 (d) [10.5] (3 H)	10.05 (d), −2.54 (d) [29.3]
	cct	2.01 (T) [8.3]	−0.79 (s)
Me$_3$P	ttt	1.70 (T) [7.8]	−9.14 (s)
	ccc	NO	4.99 (d), −9.05 (d) [31.7]
	cct	1.71 (T) [8.0]	−7.84 (s)

^{a} Positive chemical shifts are downfield of TMS. ^{b} Positive Chemical shifts are downfield of 85% H$_3$PO$_4$. ^{c} Abbreviations: s = singlet; d = doublet; t = first-order triplet; T = second-order, non-1:2:1 three-line multiplet; $J = |^2J_{PH} + {}^4J_{PH}|$, in Hz; NO = not observed; NA = not applicable. ^{d} Methylene resonance.

Table VII. ^{13}C{^{1}H} Nuclear Magnetic Resonance Data for RuCl$_2$(CO)$_2$(phosphine)$_2$ Complexes

		δ^a (mult^b) [J, Hz]	
phosphine	geometry	CH$_3$ or CH$_2$	CO
Bzl$_3$P	ttt	31.9 (T) [20.5]	NO
	cct	30.9 (T) [22.0]	191.96 (t), [10.3]
Ph$_3$P	cct	NA	192.37 (t) [11.0]
Ph$_2$MeP	ttt	14.40 (T) [33.0]	194.88 (t) [13.2]
	ccc	12.79 (d) [35.4]; 12.03 (d) [34.2]	194.71 (t) [13.2^c]; 187.94 (dd) [118.0,^{d} 9.6^e]
	cct	12.18 (T) [34.2]	192.72 (t) [10.3]
PhMe$_2$P	ttt	13.92 (T) [33.0]	194.50 (t) [13.8]
	ccc	17.45 (d) [36.6]; 14.50 (d) [35.4]	193.89 (dd) [15.5,^{f} 12.5^e]
		14.35 (d) [35.4]; 10.48 (d) [34.2]	188.00 (dd) [117.2,^{d} 9.5^e]
	cct	12.30 (T) [33.7]	192.66 (t) [10.2]
Me$_3$P	ttt	15.51 (T) [32.2]	195.23 (t) [13.9]
	ccc	19.84 (d) [35.2]; 14.99 (d) [32.2]	NO
	cct	14.87 (T) [33.7]	193.24 (t) [11.7]

^{a} All chemical shifts are referenced to the center line of CDCl$_3$ (77.00 ppm). ^{b} Abbreviations: s = singlet; d = doublet; t = first-order triplet; m = unresolved multiplet; T = second-order, non-1:2:1 three-line multiplet; $J = |^1J_{PC} + {}^3J_{PC}|$; NA = not applicable; NO = not observed. $^c J_{PC}$(cis (P trans to other CO)) = J_{PC}(cis (P trans to Cl)). $^d J_{PC}$(trans (P trans to CO)). $^e J_{PC}$(cis (P trans to Cl)). $^f J_{PC}$(cis (P trans to other CO)).
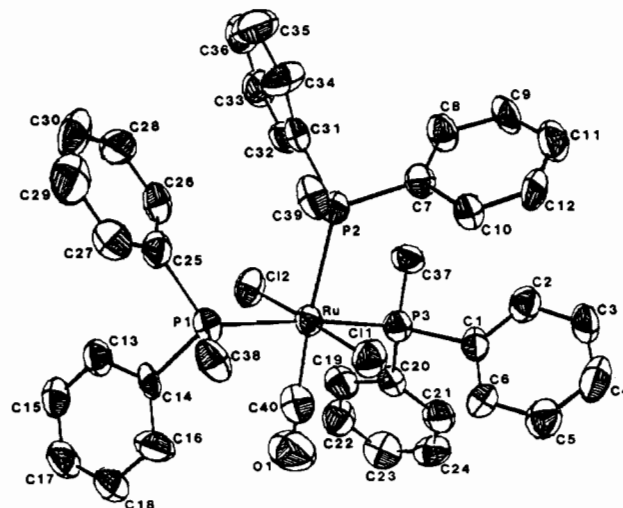
atoms were refined anisotropically, while for **1**, due to the size of the problem, all carbons were refined isotropically. Final atom coordinates of the core atoms for **1** and **2** are given in Tables IV and V, and selected bond lengths and angles are given in Figures 1 and 2.

Results and Discussion

(A) Preparation and Characterization of the Complexes. (1) Dichlorodicarbonylbis(phosphine)ruthenium(II) Complexes. Bubbling carbon monoxide through a refluxing solution of hydrated RuCl$_3$ in 2-methoxyethanol gives a product often described as "RuCl$_2$(CO)$_2$".[17] If 2 equiv of a phosphine is added to this solution, complexes I–V are possible. Each can be distinguished
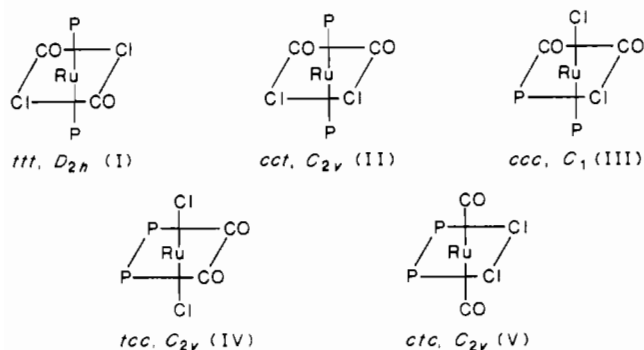
from the others by a combination of spectroscopic techniques. Observation of the C–O and Ru–Cl stretches in the infrared region along with ^{31}P{^{1}H}, ^{1}H, and ^{13}C{^{1}H} NMR uniquely define the

(17) Seddon, E. A.; Seddon, K. R. *The Chemistry of Ruthenium*; Elsevier: Amsterdam, 1984. Thomas, N. C. *Coord. Chem. Rev.* **1986**, *70*, 121.

ttt, D_{2h} (I)   *cct,* C_{2v} (II)   *ccc,* C_1 (III)

tcc, C_{2v} (IV)   *ctc,* C_{2v} (V)

Figure 2. ORTEP diagram of *trans*-(Ph$_2$MeP)$_3$Ru(CO)Cl$_2$ with 50% probability ellipsoids showing the atom-numbering scheme. Selected bond distances (in Å) are as follows: RuCl1, 2.422 (4); RuCl2, 2.423 (3); RuP1, 2.403 (4); RuP2, 2.490 (4); RuP3, 2.403 (4); RuC, 1.865 (14); CO, 1.06 (12). Selected bond angles (in degrees) are as follows: Cl1RuC2, 177.3 (1); Cl1RuP1, 89.8 (1); Cl1RuP2, 93.3 (1); Cl1RuP3, 83.5 (1); Cl1RuCl, 88.0 (4); Cl2RuP1, 87.6 (1); Cl2RuP2, 89.2 (1); Cl2RuP3, 97.4 (1); Cl2RuC, 91.2 (4); P1RuP2, 172.9 (1); P1RuP3, 92.5 (1); P1RuC, 88.0 (4); P2RuP3, 94.2 (1); P2RuC, 85.7 (4); P3RuC, 171.5 (4); RuCO, 176.3 (3).

structure of each observed product. The infrared data for these products are given in Table I and the NMR data in Tables VI and VII.

Table VIII. $^{13}C\{^1H\}$ Nuclear Magnetic Resonance Data (Phenyl Region) for $RuCl_2(CO)_2(phosphine)_2$ Complexes

phosphine	geometry	δ^a (mult^b) [J, Hz]			
		ipso	$C_{2,6}$	$C_{3,5}$	C_4
Bzl_3	*ttt*	133.98 (s)	130.53 (s)	128.60 (s)	126.90 (s)
	cct	133.98 (T) [5.9]	130.47 (s)	128.77 (s)	126.96 (s)
Ph_3P	*cct*	131.76 (T) [48.0]	134.27 (T) [10.3]	128.19 (T) [10.3]	130.53 (s)
Ph_2PMe	*ttt*	134.35 (T) [47.6]	132.17 (T) [9.8]	128.37 (T) [9.8]	130.32 (s)
	cct	133.19 (T) [46.4]	132.32 (T) [11.0]	128.56 (T) [9.8]	130.61 (s)
$PhPMe_2$	*ttt*	135.78 (T) [34.2]	127.98 (T) [9.8]	127.20 (T) [8.5]	128.61 (s)
	ccc^c	137.33 (dd) [51.4, 1.0]	130.26 (d) [7.9]^e	128.88 (d) [14.4]^e	128.80 (s)
	ccc^d	135.30 (dd) [41.6, 2.0]	130.07 (d) [15.0]^e	128.71 (d) [14.0]^e	128.80 (s)
	cct	135.97 (T) [45.5]	129.30 (T) [10.2]	128.77 (T) [8.8]	130.23 (s)

^{a} All chemical shifts are relative to the center line of $CDCl_3$ (77.00 ppm). ^{b} Abbreviations: s = singlet; d = doublet; T = second-order, non-1:2:1 three-line multiplet; $J = |^nJ_{PC} + {}^{n+2}J_{PC}|$. ^{c} Phenyl resonances for phosphine trans to chloride. ^{d} Phenyl resonances for phosphine trans to carbonyl. ^{e} Not unambiguously assigned.

(a) Trans–Trans–Trans Isomer. When 2 equiv of Bzl_3P or Ph_2MeP is added to a cooled solution of "$RuCl_2(CO)_2$" in 2-methoxyethanol, a yellow complex of composition $RuCl_2(CO)_2P_2$ precipitates directly from the solution as the lone kinetic product. The observation of single C–O and Ru–Cl vibrations in the infrared spectrum is only consistent with the all-trans (*ttt*) structure (I). Throughout this work this isomer is referred to as the *ttt* isomer, designating trans chlorides, trans carbonyls, and trans phosphine ligands.

When the $PhMe_2P$ and Me_3P complexes were prepared under similar reaction conditions, significant amounts of the tris-(phosphine) complexes were formed in addition to the bis(phosphine) complex. This is probably due to the smaller size and greater basicity of these ligands, allowing for facile displacement of another CO group. These bis- and tris(phosphine) complexes were separated by fractional crystallization from dichloromethane/ethanol. In general, the tris(phosphine) complex is the more soluble. Solubility also varies according to the phosphine, increasing in organic solvents in the sequence Bzl_3P < Ph_2MeP < $PhMe_2P$ < Me_3P for both the bis and tris complexes.

Arrangements of the CO and Cl ligand pairs as trans also establishes the phosphines to be in trans configuration. Since they are symmetry-related, only a single resonance is observed by $^{31}P\{^1H\}$ NMR. The ^{13}CO resonance appears as a triplet due to coupling to the two equivalent phosphines. The small values of $^2J_{P-CO}$ (<20 Hz) are typical of cis coupling constants.[12]

In the methyl region of the ^{13}C NMR spectra all resonances appear as 1:2:1 triplets. The resonances for the methyl protons appear as three-line multiplets, where the center line is slightly broadened. In both cases these spectra arise from a second-order effect usually referred to as "virtual coupling". The spin system for the methyl protons in the *ttt* complex, for example, is $X_nAA'X'_n$ (A, A' = ^{31}P; X, X' = ^1H). The line shapes of such virtually coupled spectra have been shown to depend on the relative magnitudes of $J_{AA'}$, J_{AX} ($=J_{A'X'}$), and $J_{A'X}$ ($=J_{AX'}$).[18,19] When $J_{AA'} < (1/2|J_{AX} - J_{A'X}|^2)\Delta\nu_{1/2}$, where $\Delta\nu_{1/2}$ is the resolving power of the instrument, the X resonance will appear as a "filled-in doublet". On the other hand, if $J_{AA'} > 2|J_{AX} - J_{A'X}|^2\Delta\nu_{1/2}$, then 1:2:1 triplets may be observed. In each case the two major outer lines in the spectrum are separated by $|J_{AX} + J_{A'X}|$. In the latter case the center line of the "triplet" may be broad if $|J_{AX} - J_{A'X}|$ is small but not zero.[20]

For Ru(II) complexes $J_{AA'}$ is usually large for mutually trans phosphines (>200 Hz)[20-24] and is much smaller when these ligands are cis (<50 Hz).[21,25,26] Furthermore, $|J_{AX} - J_{A'X}|$ is generally

less than 12 Hz. Clearly then, only the presence of trans phosphines can satisfy the conditions necessary for the observation of a "triplet". Thus, the "triplets" observed for each of the *ttt* complexes confirm that the phosphines are mutually trans.

The shape of the ^{13}C methyl resonance is not as useful in determining the orientation of the phosphine ligands as are the ^1H spectra. Because of the low natural abundance of ^{13}C, the spin system is now AA'X, where X = ^{13}C. Also, for these complexes J_{AX} is about 35 Hz and $J_{A'X}$ is small or negative, so $|J_{AX} - J_{A'X}|$ is large. As a consequence of both of these conditions we have found that smaller values of J_{PP} (ca. 50 Hz) will satisfy the conditions for the observation of a 1:2:1 triplet. The observation of 1:2:1 triplets in the ^{13}C spectra indicates that J_{PP} > 50 Hz and that the phosphines are probably mutually trans. The ^{13}C data for the phenyl carbons is given in Table VIII. With the exception of the para carbons, all the phenyl ring carbons also appear as 1:2:1 triplets, again suggesting trans phosphines. For the tribenzylphosphine complexes all the aromatic carbon resonances are singlets due to cancellation of coupling constants, $|^nJ_{PC} + {}^{n+2}J_{PC}| = 0$, and so provide no structural information.[27]

(b) Cis–Cis–Trans Isomer. Adding 2 equiv of the phosphine ligand to a refluxing 2-methoxyethanol solution of "$RuCl_2(CO)_2$" gives a near-colorless, thermodynamically stable product. The infrared spectrum shows two CO and two RuCl vibrations, indicating that both of these ligand pairs are cis. It has been shown that, for two ligands bound to a metal, the relative intensities of their symmetric and asymmetric vibrations are influenced by the angle between the ligands and that these intensities will be identical if this angle is 90°.[28]

Since the two CO absorptions are of equal intensity, this supports the idea that these ligands are in a cis orientation. As with the *ttt* complexes, the shapes of the ^1H and ^{13}C methyl resonances indicate that the phosphines are trans to each other. As expected, only one resonance is observed by $^{31}P\{^1H\}$ NMR. The thermodynamic product must thus have the cis–cis–trans (*cct*) geometry (isomer II).

(c) Cis–Cis–Cis Isomer. Mild heating (50 °C) of a chloroform solution of the *ttt* isomer (P = Bzl_3P) resulted in rapid isomerization to the *cct* complex. Successively higher temperatures were required to bring about isomerization of the *ttt*-Ph_2MeP, -$PhMe_2P$, and -Me_3P complexes, and in these cases the *cct* isomer was not the initial product. Instead an intermediate formed first, which upon further vigorous heating could be converted to the *cct* isomer. The intermediate could not be isolated in a pure state from the isomerization solution, but its structure could be determined easily in situ. Infrared spectroscopy showed two CO absorptions of equal intensity indicating cis carbonyl ligands (except for the impure Me_3P complex, where the band of lower energy was obscured by

(18) Redfield, D. A.; Nelson, J. H.; Cary, L. W. *Inorg. Nucl. Chem. Lett.* **1974**, *10*, 727.
(19) Redfield, D. A.; Cary, L. W.; Nelson, J. H. *Inorg. Chem.* **1975**, *14*, 50.
(20) Harris, R. K. *Can. J. Chem.* **1964**, *42*, 2275.
(21) Verkade, J. G. *Coord. Chem. Rev.* **1972/73**, *9*, 1.
(22) Probitts, E. J.; Saunders, D. R.; Stone, D. H.; Mawby, R. J. *J. Chem. Soc., Dalton Trans.* **1986**, 1167.
(23) Rosete, R. O.; Cole-Hamilton, D. J.; Wilkinson, G. *J. Chem. Soc., Dalton Trans.* **1984**, 2067.
(24) Bright, A.; Mann, B. E.; Masters, C.; Shaw, B. L.; Slade, R. M.; Stainbank, R. E. *J. Chem. Soc. A* **1971**, 1826.

(25) Pankowski, M.; Chodkiewicz, W.; Simonnin, M. *Inorg. Chem.* **1985**, *24*, 533.
(26) Pregosin, P. S.; Kunz, R. W. *NMR: Basic Princ. Prog.* **1979**, *16*, 28.
(27) Verstuyft, A. W.; Nelson, J. H.; Cary, L. W. *Inorg. Chem.* **1976**, *15*, 732.
(28) Cotton, F. A.; Wilkinson, G. *Advanced Inorganic Chemistry*, 4th ed.; Wiley-Interscience: New York, 1980; p 1073.

Table IX. Spectroscopic Data for [RuCl$_2$(CO)(phosphine)$_2$]$_2$ Complexes[a]

					δ (mult[c]) [J, Hz]		
						^{13}C	
phosphine	color	ν_{CO},[b] cm^{-1}	^{31}P	^{1}H	^{13}CH$_3$	^{13}CO
Bzl$_3$P	yellow	1975	39.22 (s)	3.57 (T) [7.3]	30.96 (T) [22.0]	NO
Ph$_2$MeP	yellow	1977[d]	31.43 (s)[d]	1.87 (filled-in d)[d]	e	e
PhMe$_2$P	yellow	1977	23.37 (s)	1.65 (filled-in d)	17.37 (T) [36.6]; 13.98 (T) [36.6]	197.98 (t) [19]
Me$_3$P	NI		18.35 (s)			

[a] Phosphorus and carbon spectra are proton-decoupled. Positive ^{31}P chemical shifts are downfield of 85% H$_3$PO$_4$; positive ^{1}H chemical shifts are downfield of TMS; ^{31}C chemical shifts downfield of TMS are positive and are relative to the center line of CDCl$_3$ (77.00 ppm). [b] In CHCl$_3$. [c] Abbreviations: s = singlet; d = doublet; T = non-first-order triplet, |$J_{AX} + J_{A'X}$|; t = first-order triplet; NI = not isolated; NO = not observed. [d] In C$_6$D$_6$. [e] Solubility limited.

an absorption due to the *cct* isomer). The ^{31}P{^{1}H} NMR spectra of the intermediate consisted of two doublets due to coupling of two chemically inequivalent phosphines. All the ligand pairs must be cis so that each phosphine can be trans to a different ligand. Of the structures I–V, only isomer III, referred to as the *ccc* isomer, is consistent with these observations. The measured values of $^2J_{PP}$ (<50 Hz) are also indicative of cis phosphines.

Proton and ^{13}C NMR spectra were obtained for pure samples of the *ccc* complexes of P = Ph$_2$MeP and PhMe$_2$P. Due to the low symmetry of the *ccc* isomer, each methyl group is in a unique environment with a unique chemical shift. This allows for a first-order analysis of the spectra, and each methyl resonance appears as a doublet due to $^2J_{PH}$ or $^1J_{PC}$. Thus, when P = Ph$_2$MeP, two doublets are found in both the ^{1}H and ^{13}C{^{1}H} NMR spectra. Only three doublets are seen in the proton spectrum of the PhMe$_2$P complex because two of the methyl resonances are accidentally chemical shift equivalent. Selective phosphorus decoupling of the proton spectrum allowed assignment of the downfield proton doublet to the phosphorus resonance at higher field and the upfield pair of doublets to the downfield phosphorus. This corresponds to the phosphorus nuclei trans to CO and Cl, respectively (vide infra). The collapse of each doublet to a singlet confirms that the cis four-bond P–H coupling is zero and that the observed coupling is due only to $^2J_{PH}$. The ^{13}C spectrum of the PhMe$_2$P complex showed four distinct doublets. The assignment of these carbon resonances was based upon the order of the ^{1}H chemical shifts of this complex. For the Me$_3$P complex, the three methyl groups on each phosphine are equivalent due to rotation about the M–P bond. Thus, only two doublets are observed for it, one for the methyl groups on each phosphine.

A separate resonance was observed for each ^{13}CO ligand in *ccc*-RuCl$_2$(CO)$_2$(PhMe$_2$P)$_2$. The carbonyl carbon trans to the phosphine appears as a well-separated doublet of doublets. In this case $^2J_{PC}$(trans) (117.2 Hz) $\gg$ $^2J_{PC}$(cis) (9.5 Hz). The resonance for ^{13}CO trans to chloride appears as a closely spaced doublet of doublets, since the values of the cis P–C coupling constants are only slightly different. The ^{13}C spectrum in the phenyl region (Table VIII) also shows the inequivalent nature of the two phenyl groups. Each ipso carbon resonance has a unique chemical shift and appears as a doublet of doublets due to unequal coupling to both phosphines. Both para carbon resonances are singlets with the same chemical shift, but the two ortho and meta pairs of carbons each appear as doublets.

The *ccc* isomers (P = Ph$_2$MeP, PhMe$_2$P, and Me$_3$P) are more difficult to isomerize than the *ttt* isomers. However, *ccc*-RuCl$_2$(CO)$_2$(Bzl$_3$P)$_2$ (prepared by CO cleavage of the dimer; vide infra) isomerizes much more rapidly than the all-trans complex with isomerization being complete in less than 20 min at room temperature. This explains why the isomerization of *ttt*-RuCl$_2$-(CO)$_2$(BzlP)$_2$ appears to proceed directly to the *cct* product. The isomerization rate of this *ccc* complex is large enough that it does not accumulate during the isomerization of the *ttt* complex and so is not observed.

(d) [RuCl$_2$(CO)(phosphine)$_2$]$_2$ Complexes. Dilute solutions of the *ttt*-RuCl$_2$(CO)$_2$(Ph$_2$MeP)$_2$ complex isomerize thermally to the *cct* isomer via the all-cis complex. However, when a saturated solution of the *ttt* isomer is refluxed for 7 h in chloroform, a yellow powder precipitates. If the reaction is followed by ^{31}P NMR, the

initial major product in solution is found to be the *ccc* isomer. After precipitation of the solid only a small amount of the all-cis isomer remains. The solid has been shown by Mawby[11] to be a binuclear complex with the formula [RuCl$_2$(CO)(Ph$_2$MeP)$_2$]$_2$. This dimer results from the loss of CO from 2 equiv of the *ccc* complex and combination of the coordinatively unsaturated fragments. A bimolecular reaction of this type would be expected to occur to a greater extent as the concentration of the starting complex increases.

The dimer for P = Bzl$_3$P was also prepared by refluxing the *ttt* isomer in chloroform. In this case the dimer was very soluble, and isolated yields were quite low (<6%). [RuCl$_2$(CO)-(PhMe$_2$P)$_2$]$_2$ could not be prepared by this method. Instead, this complex was isolated from a reaction in which a dilute solution of the phosphine in 2-methoxyethanol was slowly added to a refluxing 2-methoxyethanol solution of "RuCl$_2$(CO)$_2$". Passing CO through a suspension of each dimer in CHCl$_3$ at room temperature produced the all-cis complex. Pure all-cis complexes were obtained for all but the trimethylphosphine complex by this method.

The infrared and NMR spectroscopic data for the characterization of the dimers is given in Table IX. Each dimer shows only a single ^{31}P resonance, indicating that all of the phosphine ligands are symmetry-related. On the basis of this evidence and the molecular formula, structures VI–IX are possible. Dimers
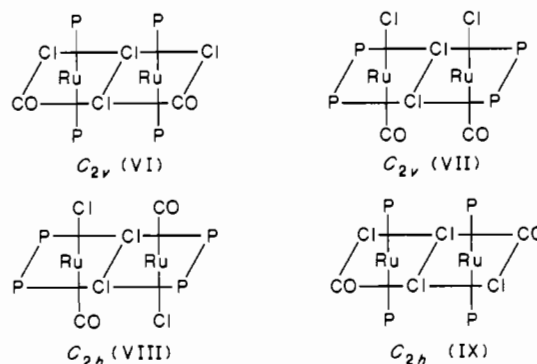
VI and VII have C_{2v} symmetry and should show two CO stretches in their infrared spectra. The complexes VIII and IX are of C_{2h} symmetry, and for them only one infrared-active CO band should be observed. Since each dimer shows only a single C–O vibration, dimers VI and VII can be eliminated as possible structures.

Proton and ^{13}C{^{1}H} NMR spectra allow assignment of either structure VIII or IX to the dimers. When P = Ph$_2$MeP and PhMe$_2$P, the methyl proton resonances appear as "filled-in doublets". In addition, two non-1:2:1 three-line multiplets are found for the methyl carbons of the PhMe$_2$P dimer. (The solubility of [RuCl$_2$(CO)(Ph$_2$MeP)]$_2$ was too low to allow for a good ^{13}C spectrum.) Both types of spectra result from coupling to two phosphines in cis positions. The ^{13}CO resonance of [RuCl$_2$-(CO)(PhMe$_2$P)$_2$]$_2$ was a 1:2:1 triplet with $^2J_{PC}$ = 20 Hz. This requires the CO ligands to be symmetry-related and to be cis to two equivalent phosphines. Thus, structure VIII is likely for the PhMe$_2$P dimer and, by inference, for the Ph$_2$MeP dimer as well. For [RuCl$_2$(CO)(Bzl$_3$P)$_2$]$_2$ trans phosphines are indicated by the

Table X. Calculated CO Force Constants (dyn/cm) for $RuCl_2(CO)_2(phosphine)_2$ Complexes

geometry	phosphine	k_f^a	k_i^a
cct	Me₃P	16.45	0.522
	PhMe₂P	16.55	0.499
	Ph₂MeP	16.58	0.491
	Ph₃P	16.63	0.492
	Bzl₃P	16.53	0.474
ccc	Me₃P	16.73	0.805
	PhMe₂P	16.80	0.684
	Ph₂MeP	16.87	0.718
	Bzl₃P	16.82	0.620

geometry	phosphine	k_f^b	$k - 2k_i$
ttt	Me₃P	(17.29)	16.25
	PhMe₂P	(17.28)	16.28
	Ph₂MeP	(17.32)	16.33
	Bzl₃P	(17.22)	16.27

^{a} As chloroform solutions. ^{b} Estimates derived by using values of k_i from *cct* isomers.

1:2:1 "triplets" that are observed in both the proton and ^{13}C methylene regions. Structure IX is consistent with this and the infrared data. This result seems unusual in light of the fact that the cleavage of this dimer with CO gives the *ccc* isomer; the *ttt* isomer might have been expected to form initially from a dimer with this structure. Furthermore, the ^{31}P chemical shift is quite downfield (about 39 ppm), even more so than the resonance for Bzl₃P trans to chloride in the corresponding *ccc* complex, and suggests that the phosphine could be trans to a bridging chloride. Because of these ambiguities, the structure of this dimer is still uncertain.

(e) Influence of the Nature of the Phosphine on the Relative Thermodynamic Stabilities. The relative stabilities of the three isomers of $RuCl_2(CO)_2P_2$ can be attributed to the relative orientation of the ligands, while the variation in lability within each group of isomers (for example the *ttt* complexes) seems to depend on the donor ability and steric bulk of the phosphine. Since the most common mechanism of reaction of metal carbonyl complexes is the initial dissociation of CO,[29] the effect of these changes on this ligand are probably the most important. Carbon monoxide binds to a metal through a combination of σ-donor (C→M) and π-acceptor (C←M) modes. Since CO is a very good π acceptor, the M–C bond strength is sensitive to changes in the overall electron density of the metal. When two CO ligands are mutually trans, they compete for electron density residing in the same metal d orbital and the amount of M→C back-bonding is reduced. Thus, CO ligands in trans positions tend to labilize each other.[30] Phosphines are generally not good π acceptors,[31] and Cl ligands are even less so, so the trans influence toward CO decreases in the order CO > P > Cl. Thus, in the *ccc* isomer the loss of CO trans to phosphine is likely to be more difficult than in the *ttt* isomer. This is reflected in the generally lower lability of the *ccc* isomer, except where the phosphine ligand is quite bulky. The M–CO bonds trans to Cl in the *cct* isomer are stronger still and probably account for this isomer being the thermodynamically preferred product.

This ordering of relative labilities may be predicted from the relative magnitudes of the C–O force constants, which have been shown to depend to a great extent on the amount of π character in the C–O bond. The force constant (k_f) and the stretch–stretch interaction constants (k_i) were calculated for the *ccc* and *cct* isomers on the basis of the energy of the two C–O absorptions by using the method of Cotton and Kraihanzel[32] (Table X). Estimates are given for k_f for the *ttt* complexes (in parentheses), since these values are based on the lone infrared-active CO stretch

and the value of k_2 for the corresponding *cct* complexes. The Ru–C and C–O bond strengths have an inverse relationship because of π back-bonding, so as the C–O bond strength decreases the Ru–C bond strength increases. Clearly then, the decrease in k_f as the geometry varies from *ttt* to *ccc* to *cct* indicates that the Ru–C bond strength increases in this same order. This correlates well with the observed labilities of these isomers, which is in general *ttt* > *ccc* > *cct*.

A regular change in k_f also occurs with the donor ability of the phosphine. As the phosphine becomes a better σ donor, more electron density is available on the metal for π back-bonding to CO, and thus k_f decreases. This is observed in the series of *ccc* and *cct* isomers as the phosphine is varied from Ph₃P to Me₃P. A similar trend is not apparent for the *ttt* isomers; perhaps it is obscured due to uncertainties in the energy of the CO stretch (±1 cm) and the use of estimates for k_i.

The decrease in k_f as the geometry changes from *ttt* to *cct* may also indicate that the phosphines are better donors in the *cct* complexes. This is supported by the ^{31}P coordination chemical shift ($\Delta\delta(^{31}P)$) of the phosphines ($\Delta\delta(^{31}P) = \delta(^{31}P)_{complex} - \delta(^{31}P)_{ligand}$), where a larger $\Delta\delta(^{31}P)$ value implies better donor ability.[33] For all the methyl phosphines the coordination chemical shift is larger in the *cct* isomers than in the *ttt* isomers.

(2) Dichlorocarbonyltris(phosphine)ruthenium(II) Complexes (Phosphine = Me₃P, PhMe₂P, Ph₂MeP). Two isomers of composition $RuCl_2(CO)P_3$ are formed if 3 mol of phosphine is added to a "$RuCl_2(CO)_2$" solution under different conditions. If the "$RuCl_2(CO)_2$" solution is cooled and 3 equiv of Me₃P or PhMe₂P is added, the yellow or orange kinetic product that forms is a complex of the type $RuCl_2(CO)P_3$. For Ph₂MeP, however, *ttt*-$RuCl_2(CO)_2(Ph_2MeP)_2$ is formed initially. In this case addition of excess phosphine is required to bring about the displacement of another CO and formation of the tris(phosphine) complex. With Ph₃P or Bzl₃P, none of the tris(phosphine) complex is formed even with excess ligand. Evidently the large size of these latter ligands makes coordination of the third phosphine difficult.

The pale yellow, thermodynamically stable isomer is obtained by adding the phosphine to a refluxing solution of "$RuCl_2(CO)_2$" in 2-methoxyethanol. Alternately, a solution of the kinetic product can be isomerized to give the thermodynamic product by refluxing in chloroform (bp 61 °C) for P = Ph₂MeP or in 2-methoxyethanol (bp 125 °C) for P = PhMe₂P, Me₃P.

In some cases it appears that the thermodynamically stable isomer can also be formed by isomerization of the kinetic isomer in the solid state. While the melting points of the two isomers of $RuCl_2(CO)(Ph_2MeP)_3$ were determined, it was noticed that the orange kinetic product turned yellow without melting in the temperature range of 168–180 °C. The yellow complex subsequently melted at a temperature corresponding to that of the thermodynamic isomer. Similarly, if orange crystals of $RuCl_2(CO)(Me_3P)_3$ were placed in an oven at 170 °C, the crystals turned a much lighter color after 10 min. A comparison of the ^{31}P NMR and infrared spectra of this complex with those of the thermodynamic product showed them to be identical. A more complete investigation of the extent of such solid-state rearrangements is reported elsewhere.[34]

There are three possible isomers (X–XII) for complexes with the formula $RuCl_2(CO)P_3$. Both X and XI have the phosphines

trans, C_{2v} (X)   cis, C_s (XI)   facial, C_1 (XII)
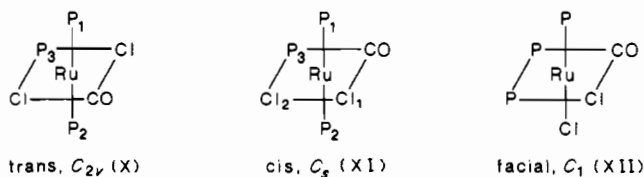
in a meridional arrangement, while in XII the phosphines are

(29) Darensbourg, D. J. *Adv. Organomet. Chem.* **1982**, *21*, 113.
(30) Chatt, J.; Shaw, B. L.; Field, A. E. *J. Chem. Soc.* **1964**, 3466.
(31) Golovin, M. N.; Rahman, M. M.; Belmonte, J. E.; Giering, W. P. *Organometallics* **1985**, *4*, 1981.
(32) Cotton, F. A.; Kraihanzel, C. S. *J. Am. Chem. Soc.* **1962**, *84*, 4432.
(33) Nelson, J. H.; Mathey, F. In *Methods of Stereochemical Analysis*; Verkade, J. G., Quin, L. D., Eds.; VCH: Deerfield Beach, FL, 1987; Vol. 8, Chapter 19.
(34) Krassowski, D. W.; Reimer, K.; LeMay, H. E., Jr.; Nelson, J. H. *Inorg. Chem.*, accompanying note in this issue.

Table XI. $^{13}C\{^1H\}$ Nuclear Magnetic Resonance Data for RuCl$_2$(CO)(phosphine)$_3$ Complexes

phosphine	geometry	δ^a (mult^b) [J, Hz^c]		CO
		CH$_3$		
Ph$_2$MeP	trans^d	11.03 (T) [30.8]	9.42 (d) [24.9]	200.14 (dt) [pc-trans, 104.0; pc-cis(ax), 14.3]
	cis	15.52 (T) [35.2]	12.65 (d) [30.3]	201.00 (dt) [pc-cis(eq), 16.1; pc-cis(ax), 11.0]
PhMe$_2$P	trans	14.47 (T) [31.7]	12.36 (d) [24.4]	199.30 (dt) [pc-trans, 105.5; pc-cis(ax), 14.7]
	cis	17.18 (d) [33.0]	15.06 (T) [33.0]	199.71 (dt) [pc-cis(eq), 16.1; pc-cis(ax), 12.3]
			13.35 (T) [33.0]	
Me$_3$P	trans	16.10 (T) [30.8]	14.93 (d) [26.4]	199.77 (dt) [pc-trans, 108.4; pc-cis(ax), 13.9]
	cis	20.69 (d) [33.7]	16.51 (T) [30.8]	198.36 (dt) [pc-cis(eq), 16.1; pc-cis(ax), 12.8]

^{a} In ppm, relative to center line of CDCl$_3$ (77.00 ppm). ^{b} Abbreviations: d = doublet; t = first-order triplet; dt = doublet of triplets; T = second-order, non-1:2:1 three-line multiplet; J = $|^1J_{PC} + {}^3J_{PC}|$. ^{c} Abbreviations: pc-trans = $^2J_{PC}$, P trans to CO; pc-cis(ax) = $^2J_{PC}$, P trans to Cl; pc-cis(eq) = $^2J_{PC}$, P trans to C. ^{d} At 0 °C.

Table XII. ^1H and $^{31}P\{^1H\}$ Nuclear Magnetic Resonance Data for RuCl$_2$(CO)(phosphine)$_3$ Complexes

phosphine	geometry	δ (mult^b) [J, Hz]		$^{31}P\{^1H\}^c$	$\Delta\delta_{AB}/J_{PP}{}^d$	^{31}P spin syst
		^1H, Me region^a				
Ph$_2$MeP	trans	1.85 (T) [6.5]	1.73 (d) [7.6]	−1.46 (d), −17.02 (t) [35.2]	17.8	AX$_2$
	cis	2.19 (T) [8.0]	1.75 (d) [9.8]	24.77 (t), 6.93 (d) [26.9]	26.6	AX$_2$
PhMe$_2$P	trans	1.69 (T) [6.7]	1.26 (d) [8.3]	−7.41 (d), −17.15 (t) [38.1]	10.3	AB$_2$
	cis	1.88 (m) [7.6]	1.21 (d) [8.3]	17.13 (t), −2.10 (d) [26.9]	28.7	AX$_2$
Me$_3$P	trans	1.58 (T) [6.7]	1.46 (d) [7.9]	−11.28 (d), −18.66 (t) [41.5]	7.2	AB$_2$
	cis	1.63 (T) [7.2]	1.59 (d) [9.4]	10.60 (t), −8.60 (d) [29.3]	26.4	AX$_2$

^{a} In ppm, positive shift downfield from TMS. ^{b} Abbreviations: d = doublet; t = triplet; m = overlapping 1:2:1 triplets; T = second-order, non-1:2:1 three-line multiplet; J = $|^2J_{PH} + {}^4J_{PH}|$. ^{c} In ppm, positive shift downfield from 85% H$_3$PO$_4$; J is J_{PP}. ^{d} For ^{31}P at 40.26 MHz, $\Delta\delta_{AB} = |\delta(^{31}P)_{doublet} - \delta(^{31}P)_{triplet}|$.

facial. Structure X is referred to as the trans complex, since in it the chloride ligands are trans to each other, and XI is designated as the cis complex.

The structures of the kinetic and thermodynamic products can be determined from their $^{13}C\{^1H\}$ and ^1H NMR spectra (Tables XI and XII, respectively) as discussed below.

(a) Trans Isomer. The ^{13}C methyl region of each kinetic product shows a 1:2:1 triplet and a 1:1 doublet. The ^1H NMR spectrum of the methyl protons also shows a doublet, in addition to a non-1:2:1 "triplet" where the center line is broadened. The doublet arises from coupling to the unique phosphine with J = $^1J_{PC}$ (or $^2J_{PH}$), while the triplet (or three-line multiplet) results from "virtual coupling" to two phosphines in trans positions. The presence of trans phosphines establishes a meridional arrangement for the three phosphine ligands.

The placement of the other ligands can be determined by the shape of the ^{13}CO resonance. We have already shown that in the *ttt*- and *cct*-RuCl$_2$(CO)$_2$P$_2$ complexes that the cis two-bond coupling of phosphorus to the carbonyl carbon is small (<20 Hz) and that a much greater coupling (>100 Hz) exists if the phosphorus and carbon nuclei are in mutually trans positions (from *ccc*-RuCl$_2$(CO)$_2$(Ph$_2$MeP)$_2$). Thus, if the kinetic products possess a CO ligand trans to a phosphine, the ^{13}CO resonance must appear as two well-separated triplets. This is indeed the case. These complexes can therefore be unambiguously assigned the trans geometry (X).

(b) Cis Isomer. Either structure XI or XII must represent the geometry of the thermodynamic product. The appearance of three-line multiplets (or "triplets") in the ^{13}C and ^1H methyl regions demonstrates that two of the phosphines are trans to each other, and only the cis structure (XI) satisfies this requirement.

For the cis isomer the ^{13}CO resonance appears as a doublet of triplets. Each phosphine ligand is cis to CO; however, slight differences exist in $^2J_{PC}$(cis) because the phosphines are in slightly different environments.

The cis complexes have lower symmetry than the trans isomers, which is reflected in the ^{13}C methyl region of *cis*-RuCl$_2$(CO)-(PhMe$_2$P)$_3$. The two methyl groups on either of the trans phosphines are diastereotopic and exhibit separate chemical shifts, and so two triplets are observed for them. In the trans isomer these methyl groups are related by a mirror plane, and so only a single triplet resonance is seen. For both isomers only one

doublet is observed for both of the methyl groups on the unique phosphine (P$_3$) since these are also related by a plane of symmetry.

The facial isomer (XII) was not isolated or detected during the synthesis of either the cis or trans isomers. Presumably this is due to the steric interactions that would result from three mutually cis phosphines. A cationic complex with facial phosphines, [RuCl(CO)(CNR)(triphos)]$^+$, has been prepared, where triphos is the tridentate ligand [(Ph$_2$PCH$_2$)$_3$CCH$_3$].[35] This geometry is evidently favored by the small "bite" of the triphos ligand, which makes it unfavorable for the phosphorus atoms to occupy meridional positions. With a longer chain tridentate phosphine, [PhP(CH$_2$CH$_2$CH$_2$PR$_2$)$_2$], a meridional arrangement is favored.[36] Only the cis and trans isomers similar to X and XI have been isolated from addition of this ligand to "RuCl$_2$(CO)$_2$" solutions.[36] Therefore, it is not surprising that the use of monodentate phosphines fails to yield any facial isomers.

(c) Phosphorus-31 NMR Spectroscopy. The ^{31}P NMR data for the monocarbonyl complexes are included in Table XII. The two types of chemical-shift-distinct phosphorus nuclei in the cis and trans isomers are best analyzed as an AB$_2$ spin system. The shape of the spectrum is affected by J_{PP} and the chemical shift difference between the different nuclei ($\Delta\delta_{AB}$). For the condition where $\Delta\delta_{AB}/J_{PP}$ < 15 (see Table XII), all eight major lines characteristic of an AB$_2$ spectrum are observed. This is the case for *trans*-RuCl$_2$(CO)(Me$_3$P)$_3$, where $\Delta\delta_{AB}/J_{PP}$ = 7.2. As this ratio increases, the spectra begin to appear as a first-order AX$_2$ case. At a value of $\Delta\delta_{AB}/J_{PP}$ = 25, first-order spectra will be seen unless the resolution of the instrument is less than 0.25 Hz. The first-order ^{31}P NMR spectra of the complexes consist simply of a 1:1 doublet and a 1:2:1 triplet with 2:1 relative intensities. For the trans complex the triplet is upfield of the doublet, while for the cis isomer this situation is reversed. The chemical shift differences of these phosphine ligand resonances not only provide an easy method for product identification but can also give insight into the relative thermodynamic stabilities of the cis and trans isomers.

It has been suggested that the chemical shift of a phosphine ligand depends on the extent to which it acts as an electron-pair

(35) Hommeltofe, S. I.; Cameron, A. D.; Shackleton, T. A.; Fraser, M. E.; Fortier, S.; Baird, M. C. *Organometallics* **1986**, *5*, 1380.
(36) Letts, J. B.; Mazanec, T. J.; Meek, D. W. *Organometallics* **1983**, *2*, 695.

Table XIII. Infrared Data for $RuCl_2(CO)(phosphine)_3$ Complexes

complex	geometry	color	ν_{CO},[a] cm^{-1}	ν_{RuCl},[b] cm^{-1}	other vibrations, cm^{-1}
$RuCl_2(CO)(Ph_2MeP)_3$	trans	orange	1991	324	
	cis	pale yellow	1955	295, 270	
$RuCl_2(CO)(PhMe_2P)_3$	trans	orange	1979	326	312, 299
	cis	pale yellow	1955	288, 277	
$RuCl_2(CO)(Me_3P)_3$	trans	orange	1981	334	341
	cis	pale yellow	1955		359, 236, 231

[a] As CHCl$_3$ solutions. [b] As CsI pellets.

donor[15,26,33] and that this donor ability can be moderated by the trans influence of the ligand opposite it.[15] A ligand with a large trans influence would weaken[37] the opposing metal–phosphorus bond, causing an upfield shift of the phosphorus resonance relative to that for a ligand with a small trans influence. On the basis of studies of chloride substitution reactions, Lupin and Shaw have proposed that the trans influence[38] in Ru(II) complexes decreases in the order P > CO > Cl. Thus, it is not surprising that for the cis isomers the $P_{1,2}$ resonance (trans to phosphine) occurs upfield of that for P_3 (trans to chloride). This implies that a stronger interacton exists between the metal and P_3 than that between the metal and either P_1 or P_2. For the trans isomer the $P_{1,2}$ resonance occurs at approximately the same chemical shift as for the cis isomer, but it is now *downfield* of the resonance due to P_3 trans to CO. This suggests that P_3 is only weakly bound to the metal and that CO has in fact a *larger* trans influence toward phosphines than either P or Cl. Dissociation of this phosphine could likely be the first step in the trans to cis isomerization, which probably proceeds in order to maximize the strength of the metal–phosphorus interactions.

The relative thermodynamic stabilities of the trans isomers can be predicted by comparing their P_3 chemical shifts with those of the free phosphines. Trimethylphosphine gives a ^{31}P resonance at –62 ppm and shifts downfield by 43 ppm upon coordination trans to CO. For dimethylphenylphosphine this downfield coordination chemical shift is not quite 30 ppm, and methyldiphenylphosphine exhibits a coordination chemical shift of only 11 ppm. Clearly, Ph$_2$MeP in the P_3 position is only a poor donor and might easily dissociate to initiate the geometric isomerization of the complex. PhMe$_2$P and Me$_3$P are better donors on both steric and electronic grounds, and so for their complexes harsher conditions are required to bring about phosphine dissociation.

(d) Infrared Spectroscopy. The infrared data for the monocarbonyl complexes are given in Table XIII. The cis and trans isomers each show only one band in the carbonyl region due to the lone CO ligand whose energy depends in part on the ligand trans to CO and, hence, on the geometry of the complex.

(e) Crystal Structures of *cis*- and *trans*-RuCl$_2$(CO)(Ph$_2$MeP)$_3$. In order to confirm the assigned structures of the two isomers, single crystals of *cis*- and *trans*-RuCl$_2$(CO)(Ph$_2$MeP)$_3$ were obtained for X-ray analyses. ORTEP diagrams showing the molecular conformations and the numbering systems of the cis and trans isomers are given in Figures 1 and 2, respectively. Two symmetry-independent molecules were found in the unit cell for the cis isomer. Since the structures are not significantly different, average values of the bond lengths and angles are used for the purpose of discussion.

Both isomers show significant distortion from a regular geometry, resulting primarily from the sterically congested environment about the unique phosphine (P3). This congestion is greater in the cis isomer because of its shorter Ru–P3 bond distance and is moderated for both isomers by an increase in the P–Ru–P bond angles to greater than 90°.

The conclusions previously drawn from NMR and infrared spectroscopy are supported by the results of the X-ray analysis. The Cl–Ru–Cl bond angles are 91.7° in the cis complex and 177.3° for the trans complex. The Ru–Cl bond distance decreases
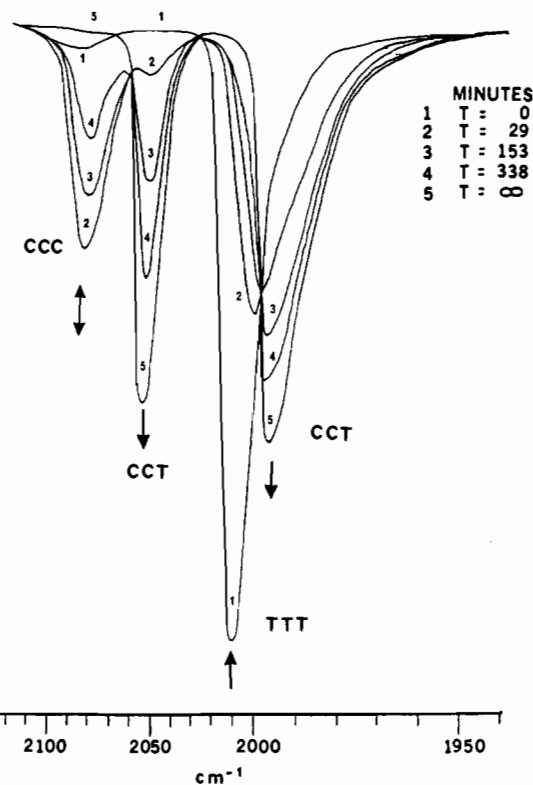

Figure 3. Change in the carbonyl region of the infrared spectrum during the thermal isomerizatin of *ttt*-(Ph$_2$MeP)$_2$Ru(CO)$_2$Cl$_2$ at 72 °C in *sym*-tetrachloroethane.

from 2.470 to 2.445 to 2.422 Å as the trans ligand is varied from P to CO to Cl. This supports the order proposed by Shaw for the trans influence of these ligands toward chloride.[15,38,39] The trans isomer contains a considerably shorter C–O bond than the cis isomer (1.06 vs 1.17 Å) and a longer Ru–C bond (1.865 vs 1.783 Å). These results are what would be expected on the basis of their relative CO stretching frequencies. In agreement with the structural assignments from ^{13}C NMR, the carbonyl ligand is trans to phosphine in the trans isomer and trans to chloride in the cis complex. Also, both complexes contain three phosphines in a meridional arrangement.

In light of the small differences between their ^{31}P chemical shifts, it is not surprising that the Ru–P1 and Ru–P2 bond lengths (2.41 Å average) are similar for the cis and trans complexes. However, in the trans isomer the resonance for P3 (trans to CO) appears far upfield, and this is reflected in a longer Ru–P3 bond (2.490 Å). The downfield chemical shift of P3 trans to Cl was proposed to result from a stronger Ru–P interaction, and this is indeed the case. The metal–phosphorus bond distance is only 2.327 Å in the cis isomer. Thus, both the ^{31}P and X-ray data confirm that the trans influence toward phosphine decreases in the sequence CO > P > Cl.

(B) Isomerizations in Solution and Activation Parameters. (1) RuCl$_2$(CO)$_2$(phosphine)$_2$ Complexes. The thermal isomerizations of the *ttt*- and *ccc*-RuCl$_2$(CO)$_2$P$_2$ complexes in solution were

(37) See: Basolo, F.; Pearson, R. G. *Mechanisms of Inorganic Reactions*; Wiley: New York, 1958; pp 172–192. Appleton, T. G.; Clark, H. C.; Manzer, L. W. *Coord. Chem. Rev.* **1973**, *10*, 335–422.
(38) Lupin, M. S.; Shaw, B. L. *J. Chem. Soc. A* **1968**, 741.

(39) See: Atwood, J. D. *Inorganic and Organometallic Reaction Mechanisms*; Brooks/Cole: Monterey, CA, 1985; pp 51–57.

**Scheme I.** Proposed Mechanism for the Isomerization of $RuCl_2(CO)_2P_2$ Complexes[a]
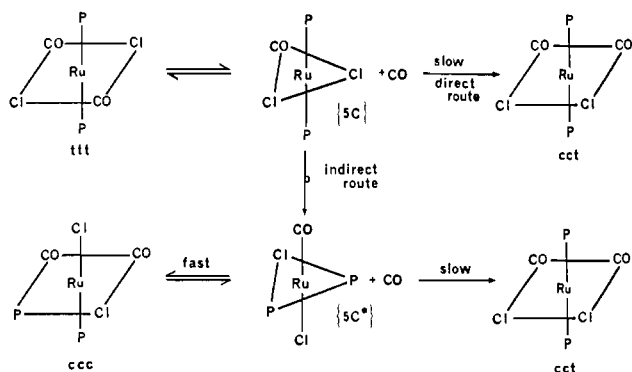
[a] Isomerization is initiated by the loss of CO. Addition of CO to 5C (direct route) is slow; the indirect route is the major path due to the high reactivity of the 5C* species. Slow dissociation of CO from the *ccc* isomer eventually gives the *cct* isomer as the final product. The geometry of the pentacoordinate species is chosen for the reasons expressed in ref 11.

followed by observing the changes in the CO stretching region of the infrared spectra. Figure 3 shows the variation of the infrared spectrum with time during the course of a typical reaction. The low-energy CO bands for the *ccc* and *cct* isomers overlap with that of the trans isomer in the 2000-cm⁻¹ region. The two high-energy bands are better separated, and changes in this region are more distinct. The initial decrease in the absorption of the *ttt* isomer is accompanied by an increase in the absorptions due to the *ccc* isomer. The absorptions due to the *ccc* intermediate then slowly decrease as those of the final *cct* product increase.

We have found that the isomerization of the *ttt* complexes is severly inhibited if the reaction is carried out under carbon monoxide pressure. Such rate inhibitions by added ligands are often indicative of a rapid preequilibrium preceding the rate-determining step. Accordingly, the mechanism of isomerization likely involves initial reversible loss of CO from the starting complex to give a coordinatively unsaturated intermediate.

Scheme I shows the mechanism proposed by Mawby for the thermal isomerization of the *ttt* complexes.[11] Loss of CO is the initial (though not necessarily the rate-determining) step, and the five-coordinate species formed initially can react in three ways: (1) reattack of CO trans to CO to give back the starting complex, (2) direct formation of the *cct* isomerization product by attack of CO trans to Cl, or (3) a Berry pseudorotation to give another 5C (five-coordinate) species, which leads to the *ccc* isomer. The extent of re-formation of the *ttt* isomer is probably large, since CO is a good trans-directing ligand. In support of this, the rate of isomerization of *ttt*-$RuCl_2(CO)_2(PhMe_2P)_2$ is 10^3 times slower than the substitution of CO by excess phosphine,[40] where the reattack of CO is negligible.

Examination of the isomerization of the *ttt* complexes (P = Me_3P, $PhMe_2P$, and Ph_2MeP) shows that these complexes isomerize to the *cct* isomer mainly by way of the *ccc* isomer, referred to as the indirect pathway (see Figure 4, supplementary material). According to Scheme I, addition of CO will not affect the direct route of isomerization,[40] but it will retard the formation of the *ccc* isomer by the indirect route. Thus, it is not surprising that under CO pressure very little of the *ccc* isomer is formed and that the rate of isomerization of the *ttt* complexes is much slower. Unlike the other complexes, very little of the *ccc* isomer is observed during the isomerization of *ttt*-$RuCl_2(CO)_2(Bzl_3P)_2$. Figure 5 (supplementary material), which shows the changes in the carbonyl region during the isomerization of this complex, indicates that only the *ttt* and *cct* isomers exist to a measurable extent during the rearrangement. This might lead one to believe that the direct path is the major route of isomerization of this complex. However,
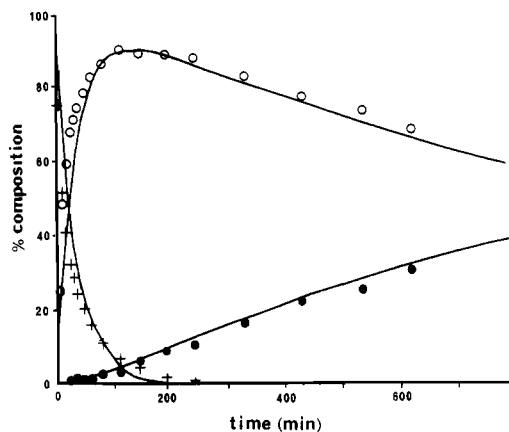
Figure 6. Experimental and calculated percent isomer composition for the thermal isomerization of *ttt*-$(Ph_2MeP)_2Ru(CO)_2Cl_2$ at 61 °C in chlorobenzene: (+) *ttt* isomer; (●) *cct* isomer; (O) *ccc* isomer. Solid lines show concentrations calculated from the equations given in ref 11 with $k_1 = 4.65 \times 10^{-4}$ s⁻¹; $k_2 = 1.13 \times 10^{-5}$ s⁻¹, and $k_4 = 0$.
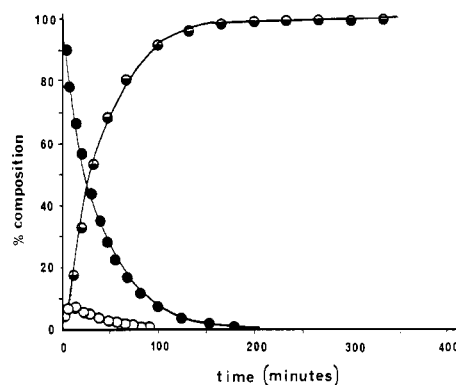

Figure 7. Possible percent isomer composition during the thermal isomerization of *ttt*-$(Bzl_3P)_2Ru(CO)_2Cl_2$: (●) *ttt* isomer; (◓) *cct* isomer; (O) *ccc* isomer. The lines are used merely to connect the calculated points. Concentrations were calculated from the equations given in ref 11 with $k_1 = 4.35 \times 10^{-4}$ s⁻¹ (experimentally observed) and k_2 arbitrarily set to $10k_1$.

added CO completely inhibits its rearrangement, and so this *ttt* isomer must isomerize almost entirely by the indirect route. The lability of the *ccc* isomer, noted earlier, precludes its observation.

The isomerization of the *ccc* complexes also appears to proceed by initial loss of CO. Mawby[11] has shown by ligand substitution reactions on *ccc*-$RuCl_2(CO)_2(PhMe_2P)_2$ that the CO ligand trans to phosphine is easily replaced. Furthermore, very concentrated solutions of *ccc*-$RuCl_2(CO)_2(Ph_2MeP)_2$ form the [$RuCl_2(CO)$-$(Ph_2MeP)_2]_2$ dimer quite easily at room temperature, also by loss of CO. Hence, dilute solutions of the *ccc* isomers that quantitatively isomerize to the *cct* isomer probably do so by loss of CO.

Both the direct and indirect pathways lead irreversibly to the *cct* isomer. By combination of both of these routes the overall rearrangement can be represented by (1). The integrated form

$$ttt \xrightarrow{k_1} ccc \xrightarrow{k_2} cct \qquad (1)$$
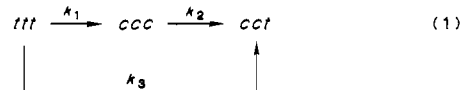
of the rate expression for this type of kinetic scheme, which has been solved by Alberty and Miller,[41] allows the calculation of the instantaneous concentrations of all species if the rate constants are known. Figure 6 shows the measured concentrations of the three isomers during the isomerization of *ttt*-$RuCl_2(CO)_2$-$(Ph_2MeP)_2$ as well as the calculated concentrations of the three isomers with values of k_1 and k_2 derived from experimental results (vide infra). Here k_1 and k_2 are the observed rate constants for

(40) Mawby, R. J. *J. Chem. Soc., Dalton Trans.* **1976**, 953 (Suppl. No. 21 718 (2 pages)).

(41) Alberty, R. A.; Miller, W. G. *J. Chem. Phys.* **1957**, *26*, 123.

Table XVI. Activation Parameters for the Isomerization of $RuCl_2(CO)_2(phosphine)_2$ Complexes

complex	isomerizn	$\Delta H^{\ddagger}$, kcal/mol	$\Delta S^{\ddagger}$, eu	$\Delta G_{373}^{\ddagger}$, kcal/mol[d]	$\Delta V^{\ddagger}$, mL/mol
$RuCl_2(CO)_2(Bzl_3P)_2$	*ttt–cct*[c]	30.1 ± 0.5	$+13 \pm 2$	25.3	
$RuCl_2(CO)_2(Ph_2MeP)_2$	*ttt–ccc*[c]	27.0 ± 1.0	$+5 \pm 3$	25.1	$+19 \pm 2$
	ccc–cct[b]	25.7 ± 1.0	-5 ± 4	27.6	
$RuCl_2(CO)_2(PhMe_2P)_2$	*ttt–ccc*[a]	27.2 ± 1.0	$+1 \pm 4$	26.8	$+19 \pm 2$
	ccc–cct[b]	22.8 ± 0.5	-19 ± 3	29.9	
$RuCl_2(CO)_2(Me_3P)_2$	*ttt–ccc*[a]	25.7 ± 1.0	-6 ± 10	28.0	

[a] In chlorobenzene. [b] In tetrachloroethane. [c] In chloroform. [d] Uncertainties in $\Delta G^{\ddagger}$ (probably ± 1 kcal/mol) are less than would be obtained by direct calculation using the uncertainties in $\Delta H^{\ddagger}$ and $\Delta S^{\ddagger}$, as variations in these last two measurements usually act to cancel, leaving $\Delta G^{\ddagger}$ little changed.

the loss of the *ttt* and *ccc* isomers, respectively. If the direct rate constant k_3 is less than 5% of k_1, then a good fit was obtained to the experimental data. At higher values of k_3 the amount of the *cct* isomer formed initially becomes significantly greater than that found experimentally. Thus, the contribution of the direct route to this isomerization is probably less than 5% when the reaction is performed without added carbon monoxide. Figure 7 shows the calculated results if $k_2 \gg k_1$ and $k_3 = 0$, as is likely for the isomerization of the Bzl_3P complexes. Note that only a very small amount of the *ccc* isomer is present at any time, and this agrees with what was found experimentally for the isomerization of *ttt*-$RuCl_2(CO)_2(Bzl_3P)_2$.
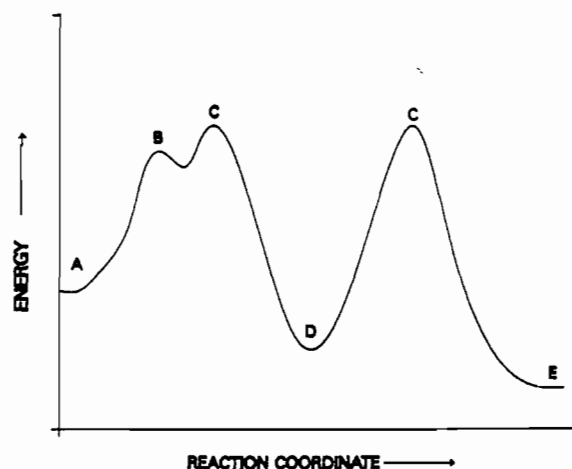
The rates of thermal isomerization of the *ttt* complexes were also measured by visible spectroscopy. Table XIV (supplementary material) lists the wavelengths of their absorption maxima and the approximate extinction coefficients. Initial rates of isomerization were measured for different concentrations of starting complex, and the linear relationship that was found between the initial rates and concentrations indicates a first-order dependence on the starting complex (Table XV, supplementary material). In addition, plots of ln (*ttt* absorbance) vs time were linear past 2 half-lives, confirming that the rearrangements are first-order with respect to the *ttt* isomers. The slopes of these plots give the observed rate constant, k_{obs}.

A modified Eyring plot (ln (k/T) vs $1/RT$) using rate constants obtained at different temperatures allowed us to calculate the activation parameters $\Delta H^{\ddagger}$, $\Delta S^{\ddagger}$, and $\Delta G^{\ddagger}$ (Table XVI). As expected, the values of $\Delta G^{\ddagger}$ decrease as the difficulty of isomerization decreases. Since the values of $\Delta H^{\ddagger}$ *increase* with the ease of isomerization, the decrease in $\Delta G^{\ddagger}$ must be due entirely to an increase in the values for $\Delta S^{\ddagger}$ as the phosphine becomes larger. Chalk and Pomeroy[42] found a similar positive relationship between the size of the phosphine ligand in $Ru(CO)_3(P)(SiCl_3)_2$ complexes and the ease of CO substitution.

Large positive values of $\Delta S^{\ddagger}$ can usually be interpreted in terms of a dissociative mechanism,[43–45] and so the small or negative values of $\Delta S^{\ddagger}$ for the rearrangement of the *ttt* isomers do not give much information about the mechanism of isomerization. However, Table XVI also gives two volumes of activation, and in these cases the large positive values indicate[46] a mechanism that is primarily dissociative in nature.

The isomerizatin of the *ccc* complexes was followed by infrared spectroscopy. Even though the uncertainties are larger, the sign of $\Delta S^{\ddagger}$ indicates the possible importance of an associative step in the rate-determining step. This step may be the addition of CO trans to Cl in the 5C* species, which is expected[40] to be slow due to the small trans-directing ability of chloride.

A possible energy profile for the *ttt* → *ccc* → *cct* isomerization of $RuCl_2(CO)_2(Ph_2MeP)_2$ is shown in Figure 8. The initial dissociation of CO trans to CO forms the five-coordinate species B, which then rearranges to the 5* species C by overcoming a small energy barrier. Subsequent addition of CO trans to phosphine
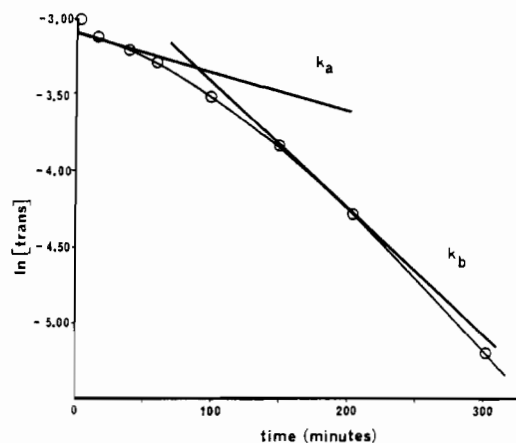
(42) Chalk, K. L.; Pomeroy, R. K. *Inorg. Chem.* **1984**, *23*, 444.
(43) Wilkins, R. G. *The Study of Kinetics and Mechanism of Reactions of Transition Metal Complexes*; Allyn and Bacon: Boston, MA, 1974.
(44) Brown, T. L.; Ludwick, L. M.; Stewart, R. S. *J. Am. Chem. Soc.* **1972**, *94*, 384.
(45) Linck, R. G. *Inorg. Chem.* **1969**, *8*, 1016.
(46) Swaddle, T. W. *Coord. Chem. Rev.* **1974**, *14*, 217.

Figure 8. Energy diagram for the isomerization of *ttt*-$(Ph_2MeP)_2Ru(CO)_2Cl_2$. Free energies of activation were determined from solution-state kinetics. The energy difference (ΔH) between the *ccc* and *cct* isomers was estimated from a DSC curve.[34] See text for an explanation of the symbols.

Scheme II. Proposed Mechanism for the Isomerization of $RuCl_2(CO)P_3$ Complexes[a]
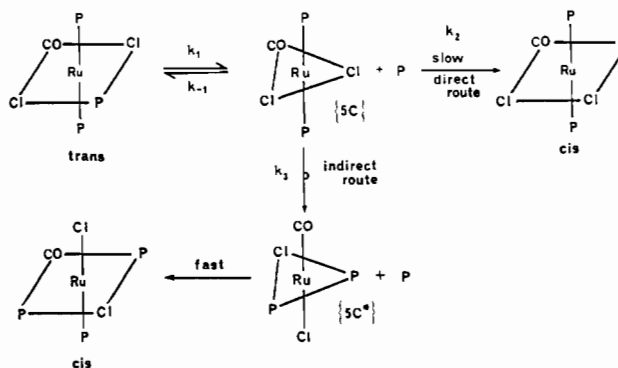
[a] Isomerization is initiated by loss of phosphine trans to CO. The cis isomer is produced mainly by the indirect route, since $k_3 > k_2[P]$.

is faster to give the *ccc* isomer D. According to the principle of microscopic reversibility, dissociation of CO from D will give the same 5C* species C. Attack of CO trans to Cl is slow to give the *cct* isomer E. The free energies of activation for both the *ttt* → *ccc* and the *ccc* → *cct* rearrangements were found from solution-state kinetics. The enthalpy difference between the *ccc* (D) and *cct* (E) isomers was estimated from the DSC curve[34] of *ccc*-$RuCl_2(CO)_2(Ph_2MeP)_2$.

(2) $RuCl_2(CO)(phosphine)_3$ Complexes. The trans to cis thermal isomerization of the $RuCl_2(CO)P_3$ complexes has been noted during the preparation and isolation of the kinetic products. A two-pathway mechanism is possible, similar to that already discussed for the geometric isomerization of the *ttt*-$RuCl_2(CO)_2P_2$ complexes, but cannot be detected directly since each pathway now gives the same cis product (Scheme II). A rate law derived from this mechanism, assuming a reversible first step followed

Figure 10. First-order kinetics plot for the thermal isomerization of *trans*-(PhMe$_2$P)$_3$Ru(CO)Cl$_2$ at 65 °C in *sym*-tetrachloroethane. The slopes of the tangents to the curve represent the observed rate constants at those points. Note that k_{obs} increases as the extent of the reaction increases; $k_b > k_a$.

Figure 11. Experimental (open circles) and calculated (solid line) dependence of k_{obs} on added Ph$_2$MeP for the isomerization of *trans*-(Ph$_2$MeP)$_3$Ru(CO)Cl$_2$ at 55 °C in chlorobenzene. The line is from curve fitting to eq 3 using the starred points.

by a slow, irreversible step for each pathway, is given in eq 2. The k_{obs} value for the reaction is given in eq 3. The thermal isom-

$$\text{rate} = \frac{-d[\text{trans}]}{dt} = \frac{d[\text{cis}]}{dt} = \frac{k_1 k_3 [\text{trans}] + k_1 k_2 [\text{trans}][\text{phosphine}]}{k_3 + (k_{-1} + k_2)[\text{phosphine}]} \quad (2)$$

$$k_{obs} = \frac{k_1 k_3 + k_1 k_2 [\text{phosphine}]}{k_3 + (k_{-1} + k_2)[\text{phosphine}]} \quad (3)$$

erization of the trans complexes could be followed by infrared spectroscopy. Figure 9 (supplementary material) shows the loss of the trans isomer along with the simultaneous formation of the cis product as a function of time. The presence of an isosbestic point indicates that no other carbonyl-containing species are involved as intermediates.

Because the trans complexes are colored and the cis isomers are nearly colorless, the isomerization could also be followed by visible spectroscopy. This method was easier than following the reaction by infrared spectroscopy, so the experiments discussed forthwith refer to data obtained by visible spectroscopic monitoring of the reactions.

The isomerization of *trans*-RuCl$_2$(CO)(PhMe$_2$P)$_3$ was investigated, and it was found not to be simply first-order in complex. Plots of ln (trans absorbance) vs time (Figure 10) showed distinct curvature, even though a linear Beer–Lambert relationship existed between absorbance and concentration. Since the tangent to the curve at any point is k_{obs}, it can be seen that as the isomerization progresses and the trans concentration decreases the value of k_{obs} increases. Similar behavior was observed for the Me$_3$P complex.

A variation in k_{obs} was confirmed by initial rate studies. Rates of isomerization were measured for six different starting concentrations of *trans*-RuCl$_2$(CO)(PhMe$_2$P)$_3$. Values of k_{obs} were calculated at the same time (t) in each reaction and are listed in Table XVII (supplementary material). With each decrease in the trans concentration the value of k_{obs} increased.

According to eq 3, any changes in k_{obs} must arise from changes in the phosphine concentration. The only source of phosphine is from ligand dissociation from the trans complex. This amount must become smaller as the isomerization progresses, allowing the numerator of expression 3 to increase relative to the denominator. The extent to which these changes in phosphine concentration will influence k_{obs} depends on the relative magnitudes of k_{-1} and k_2. When $k_{-1} \gg k_2$, then the variation in k_{obs} will be large. Since both *trans*-RuCl$_2$(CO)(PhMe$_2$P)$_3$ and *trans*-RuCl$_2$(CO)(Me$_3$P)$_3$ showed this type of behavior, this is probably true for both of these complexes. However, the isomerization of *trans*-RuCl$_2$(CO)(Ph$_2$MeP)$_3$ gave linear first-order plots of ln [trans] vs time, and initial rate studies showed a simple first-order
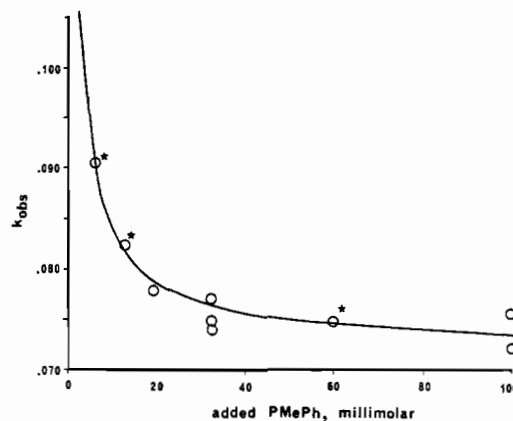
dependence on the trans complex (Table XV, supplementary material). Evidently k_{-1} is small enough for this complex that any ligand present from dissociation has only a minor effect on the observed rate constant.

The validity of these arguments was tested by carrying out the isomerizations in the presence of varying amounts of added phosphine under nitrogen. Values of k_{obs} were determined from first-order plots, but now these were linear for RuCl$_2$(CO)(PhMe$_2$P)$_3$ to well past 3 half-lives. Tables XVIII and XIX (supplementary material) show the dependence of k_{obs} on added phosphine for the isomerizations of the *trans*-RuCl$_2$(CO)(Ph$_2$MeP)$_3$ and *trans*-RuCl$_2$(CO)(PhMe$_2$P)$_3$ complexes, respectively. With use of determinants,[47] a curve was fitted to eq 3 by using the experimental points marked by asterisks. This also allowed us to derive relative values of k_{-1}, k_2, and k_3. The calculated curves are plotted along with the actual data in Figures 11 and 12 (Figure 12 is in the supplementary material), and the values for the calculated rate constants are listed in Table XX (supplementary material).

In both cases the value of k_{obs} is largest with no added phosphine and is approximated by k_1. As the amount of added phosphine increases, k_{obs} decreases to a constant value equal to $k_1 k_2/(k_{-1} + k_2)$. The effect of phosphine on isomerization is much more pronounced for the PhMe$_2$P complex. Small amounts of added phosphine brought about the maximum decrease in k_{obs}, to 12% of the value without added phosphine. This is a result of the large value of k_{-1} relative to k_2. For the Ph$_2$MeP complex k_{-1} is approximately equal to k_2, and the isomerization of this complex is relatively insensitive to the effect of added phosphine. In this case k_{obs} only decreases to 73% of its original value and requires much greater amounts of added ligand. (Similar experiments were not carried out with *trans*-RuCl$_2$(CO)(Me$_3$P)$_3$, since any added Me$_3$P (bp 38 °C) would volatilize quickly at the high temperatures required for isomerization.)

The good fit of both sets of data to expression 3 strongly supports the idea that the trans complexes undergo isomerization by loss of phosphine as suggested by Scheme II. With no added phosphine the indirect path is most important, although the direct pathway does contribute due to a small concentration of phosphine arising from its dissociation from the trans complex.

An estimate of the amount of free phosphine was made by monitoring the isomerization of *trans*-RuCl$_2$(CO)(PhMe$_2$P)$_3$ by ^{31}P NMR. No decrease in the magnitude of P–P coupling was observed at 106 °C; hence, exchange of phosphine was slow enough to allow detection of dissociated phosphine at this temperature. However, no resonance was observed at the chemical shift of PhMe$_2$P. Signal-to-noise measurements indicate that less than 0.5% of total phosphorus was present as free phosphine. This

(47) Krassowski, D. W. Ph.D. Dissertion, University of Nevada, Reno, NV, 1987.

Table XXI. Activation Parameters for the Isomerization of *trans*-RuCl$_2$(CO)(phosphine)$_3$ Complexes

phosphine	ΔH^*, kcal/mol	ΔS^*, cal/(mol K)	ΔG_{373}^*, kcal/mol	ΔV^*, mL/mol
Ph$_2$MeP^a	28.5 ± 0.5	+14 ± 2	23.8 ± 0.5	+15 ± 2
PhMe$_2$P^b	31.2 ± 0.5	+15 ± 2	26.1 ± 0.5	+16 ± 2
Me$_3$P^c	31.0 ± 0.5	+8 ± 2	28.0 ± 0.5	

^{a} In chloroform. ^{b} In 1,1,2,2-tetrachloroethane. ^{c} In chlorobenzene.

corresponds to a phosphine concentration of less than 1.5×10^{-5} M.

The relative *rates* of each pathway can now be compared by using this estimate of the free ligand concentration. Multiplying the second-order rate constants k_{-1} and k_2 by the amount of free phosphine allows a direct comparison to the first-order rate constant, k_3. These values are given in Table XX (supplementary material) relative to k_3.

For each complex the indirect pathway of isomerization (k_3) dominates over the direct path (k_2), and the extent of this difference is greater for the Ph$_2$MeP complex. Presumably the larger size of this ligand acts to hinder its attack on the five-coordinate species, 5C, as it must "squeeze" between the two phosphine ligands in trans positions. Instead, rearrangement occurs to the 5C* species, where the approach of the incoming ligand is much less sterically hindered. For the PhMe$_2$P complex, the phosphine is smaller and is a better base. The direct attack upon the 5C species is not as unfavorble, although the major path is still that of rearrangement to the 5C* species.

Activation parameters for the isomerization of the *trans*-RuCl$_2$(CO)P$_3$ complexes without added ligand were obtained either by following the rearrangement by visible spectroscopy or by observing the CO region of the infrared spectrum. For P = Ph$_2$MeP values of k_{obs} were found from the slope of the first-order plots of ln [trans] vs time. For P = PhMe$_2$P and Me$_3$P, k_{obs} was estimated by taking the tangent to the ln [trans] vs time curve at 1 half-life. Values of ΔH^* and ΔS^* were obtained from Eyring plots and ΔV^* from the pressure dependence of k_{obs} (Table XXI). In each case the large positive values of ΔS^* and ΔV^* suggest that

the isomerization proceeds by a dissociative mechanism. The calculated values of ΔG^* reflect the increasing difficulty of isomerization as the phosphine becomes smaller and a better ligand.

Conclusions

Both the *trans*-RuCl$_2$(CO)P$_3$ and *ttt*-RuCl$_2$(CO)$_2$P$_2$ complexes isomerize by ligand dissociation according to the same general mechanism. Initial loss of a phosphine ligand trans to CO occurs for the monocarbonyl complexes. The relative rates of this dissociation probably reflect a combination of steric and electronic effects. The larger, less basic ligand (Ph$_2$MeP) is only weakly bound to the metal and is easily lost. As the phosphine becomes smaller and more basic (PhMe$_2$P, Me$_3$P), the Ru–P bond becomes stronger and ligand dissociation occurs more slowly.

For the dicarbonyl complexes isomerization is initiated by the loss of a CO ligand trans to CO. Here again, the rate of isomerization decreses with a decrease in the steric bulk of the neighboring phosphine. An increase in the value of ΔS^* for the rearrangement as the phosphine becomes larger suggests the importance of steric effects on the rate of complex isomerization. However, electronic effects are also important.

Supplementary Material Available: Tables of kinetic measurements (Table II), crystal and refinement data (Table IIIS), final positional parameters (Tables IVS and VS), bond lengths and angles, and visible absorption maxima (Table XIV), a description of rate measurement techniques, tables of isomerization rates (Tables XV and XVII–XX), figures showing the percent isomer composition during isomerization of *ttt*-(Ph$_2$MeP)$_2$Ru(CO)$_2$Cl$_2$ (Figure 4), the change in the carbonyl region of the IR spectra during isomerization of *ttt*-(Bzl$_3$P)$_2$Ru(CO)$_2$Cl$_2$ (Figure 5) and *trans*-(Ph$_2$MeP)$_3$Ru(CO)Cl$_2$ (Figure 9), and the experimental and calculated dependence of k_{obs} on added PhMe$_2$P (Figure 12), and listings of thermal parameters (17 pages); listings of observed and calculated structure factors (18 pages). Ordering information is given on any current masthead page.

Notes

Contribution from the Department of Chemistry, University of Nevada, Reno, Nevada 89557

Solid-Phase Thermal Isomerization of (R$_3$P)$_2$Ru(CO)$_2$Cl$_2$ and (R$_3$P)$_3$Ru(CO)Cl$_2$ Complexes

Daniel W. Krassowski, Karl Reimer, H. E. LeMay, Jr., and John H. Nelson*

In the course of the Characterization[1] of a series of (R$_3$P)$_2$Ru(CO)$_2$Cl$_2$ (R$_3$P = Bzl$_3$P, Ph$_3$P, Ph$_2$MeP, PhMe$_2$P, Me$_3$P) and (R$_3$P)$_3$Ru(CO)Cl$_2$ (R$_3$P = Ph$_2$MeP, PhMe$_2$P, Me$_3$P) complexes, we observed that some of these complexes appeared to undergo geometrical isomerization in the solid state. Solid-state rearrangements are well-known for L$_2$PtX$_2$ complexes[2-7] (L =

neutral donor ligand, X = halide) and for cobalt(III) and chromium(III) complexes,[8] but there is very little knowledge of such solid-phase reactions of six-coordinate ruthenium(II) complexes. Therefore, an investigation of this series of *trans*-(R$_3$P)$_3$Ru(CO)Cl$_2$ and *ttt*-(R$_3$P)$_2$Ru(CO)$_2$Cl$_2$ complexes was undertaken using thermal gravimetric analysis (TGA) and differential scanning calorimetry (DSC). It was of special interest to determine if a relationship exists between the size of the phosphine and the thermal stability of the complex. The rate of geometric isomerization of these complexes in solution increases with an increase in the size of the phosphine.

Experimental Section

The complexes were prepared, characterized, and analyzed as previously described.[1] Differential scanning calorimetry and thermogravimetric analyses were obtained on 2–10-mg samples under flowing nitrogen at a constant heating rate of 20 °C/min with a Perkin-Elmer Model 2000 DSC and TGA instrument coupled with a Model 3500

(1) Krassowski, D. W.; Nelson, J. H.; Brower, K. R.; Hauenstein, D.; Jacobson, R. A. *Inorg. Chem.*, accompanying article in this issue.
(2) Ellis, R.; Weil, T. A.; Orchin, M. *J. Am. Chem. Soc.* 1970, *92*, 1078.
(3) Kukushkin, Y. N.; Budanova, V. F.; Sedove, G. N.; Pogareva, V. G.; Fadeev, Y. V.; Soboleva, M. S. *Zh. Neorg. Khim.* 1976, *21*, 1265; *Russ. J. Inorg. Chem. (Engl. Transl.)* 1976, *21*, 689.
(4) Sedova, G. N.; Demchenko, L. N. *Zh. Neorg. Khim.* 1981, *26*, 435; *Russ. J. Inorg. Chem. (Engl. Transl.)* 1981, *26*, 234.
(5) Kukushkin, Y. N.; Budanova, V. F.; Sedova, G. N.; Pogareva, V. G. *Zh. Neorg. Khim.* 1977, *22*, 1305; *Russ. J. Inorg. Chem. (Engl. Transl.)* 1977, *22*, 710.
(6) Kukushkin, Y. N.; Sedova, G. N.; Antonov, P. G.; Mitronina, L. N. *Zh. Neorg. Khim.* 1977, *22*, 2785; *Russ. J. Inorg. Chem. (Engl. Transl.)* 1977, *22*, 1512.
(7) Andronov, E. A.; Kukushkin, Y. N.; Lukicheva, T. M.; Kunovalou, L. V.; Bakhireva, S. I.; Postnikova, E. S. *Zh. Neorg. Khim.* 1976, *21*, 2443; *Russ. J. Inorg. Chem. (Engl. Transl.)* 1976, *21*, 1343.
(8) LeMay, H. E., Jr. In *Comprehensive Coordination Chemistry*; Wilkinson, G., Ed.; Pergamon: Oxford, England, 1987; Vol. 1, Chapter 8, pp 463–473.